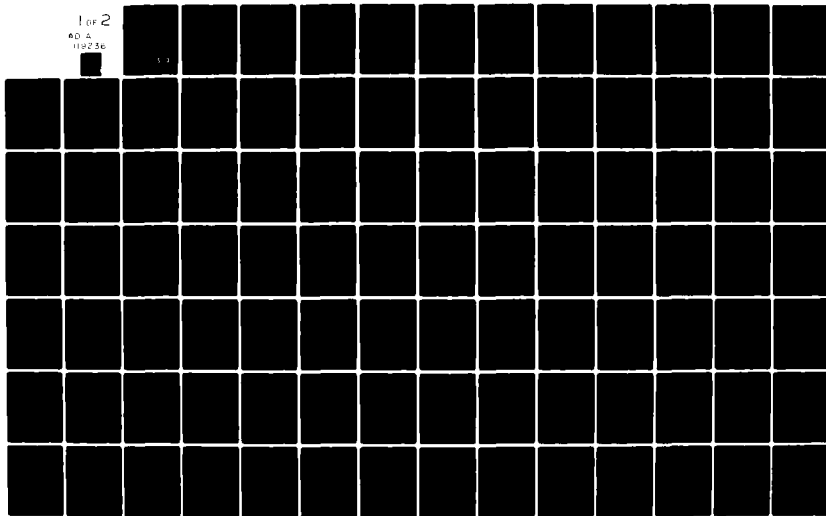


AD-A119 236

PENNSYLVANIA STATE UNIV UNIVERSITY PARK APPLIED RESE--ETC F/8 17/2
DETECTION OF A DUAL CHANNEL DIFFERENTIAL PHASE MODULATED SIGNAL--ETC(U)
JUN 82 C C MERCHANT N00024-79-C-6043
UNCLASSIFIED ARL/PSU/TM-82-136 NL

1 of 2

AD A
119236



AD A119236

6

DETECTION OF A DUAL CHANNEL DIFFERENTIAL PHASE
MODULATED SIGNAL IN CORRELATED NOISE

Clifton C. Merchant

Technical Memorandum
File No. TM 82-136
June 8, 1982
Contract No. N00024-79-C-6043

Copy No. 7

The Pennsylvania State University
Intercollege Research Programs and Facilities
APPLIED RESEARCH LABORATORY
Post Office Box 30
State College, PA 16801

APPROVED FOR PUBLIC RELEASE
DISTRIBUTION UNLIMITED

NAVY DEPARTMENT

NAVAL SEA SYSTEMS COMMAND

DTIC
ELECTE
SEP 13 1982
B

DTIC FILE COPY

00 02 13 102

UNCLASSIFIED

SECURITY CLASSIFICATION OF THIS PAGE (When Data Entered)

REPORT DOCUMENTATION PAGE		READ INSTRUCTIONS BEFORE COMPLETING FORM
1. REPORT NUMBER TM 82-136	2. GOVT ACCESSION NO. AD-A119236	3. RECIPIENT'S CATALOG NUMBER
4. TITLE (and Subtitle) Detection of a Dual Channel Differential Phase Modulated Signal in Correlated Noise		5. TYPE OF REPORT & PERIOD COVERED M.S. Thesis, August 1982
		6. PERFORMING ORG. REPORT NUMBER TM 82-136
7. AUTHOR(s) Clifton C. Merchant		8. CONTRACT OR GRANT NUMBER(s) N00024-79-C-6043
9. PERFORMING ORGANIZATION NAME AND ADDRESS The Pennsylvania State University Applied Research Laboratory, P. O. Box 30 State College, PA 16801		10. PROGRAM ELEMENT, PROJECT, TASK AREA & WORK UNIT NUMBERS
11. CONTROLLING OFFICE NAME AND ADDRESS Naval Sea Systems Command Department of the Navy Washington, DC 20362		12. REPORT DATE June 8, 1982
		13. NUMBER OF PAGES 119 pages
14. MONITORING AGENCY NAME & ADDRESS (If different from Controlling Office)		15. SECURITY CLASS. (of this report)
		15a. DECLASSIFICATION/DOWNGRADING SCHEDULE
16. DISTRIBUTION STATEMENT (of this Report) Approved for public release distribution unlimited Per Naval Sea Systems Command Aug. 9, 1982.		
17. DISTRIBUTION STATEMENT (of the abstract entered in Block 20, if different from Report)		
18. SUPPLEMENTARY NOTES		
19. KEY WORDS (Continue on reverse side if necessary and identify by block number) thesis, signal, detection, receiver, phase, difference		
20. ABSTRACT (Continue on reverse side if necessary and identify by block number) The signal detection characteristics of a two input channel receiver is studied. The signals received on both channels are random Gaussian, narrow-band processes identical except for a known channel-to-channel time delay. For narrowband representation, the time delay is treated as a differential phase modulation of the two signals. The noises on each of the two receiver channels are also random Gaussian, processes which are jointly wide sense stationary and correlated. The receiver detects the presence of a signal by estimating the average phase difference between samples of the observed signals.		

DD FORM 1473

JAN 73

EDITION OF 1 NOV 65 IS OBSOLETE

Unclassified

SECURITY CLASSIFICATION OF THIS PAGE (When Data Entered)

UNCLASSIFIED

SECURITY CLASSIFICATION OF THIS PAGE(When Data Entered)

The average phase is an input to a matched filter detector where the filter is matched to the known phase between the input signals. The receiver is intended to detect at signal-to-noise ratios less than 0 dB and over a wide range of noise correlation conditions.

The theoretical statistics required to predict the detection performance are developed. The receiver operating characteristic curves are generated for two possible signal phase functions, a sinusoidal phase shift and a linear phase shift. The results of a computer simulation of the receiver show very good agreement with the theoretical predictions.

The performance of the signal phase matched filter receiver is compared with a cross correlation receiver which includes a noise decorrelator and signal phase compensator. The cross correlation receiver is more sensitive than the signal phase matched filter receiver if the noise correlation is known. However, if the noise correlation is unknown and the detection is made using fixed signal processing and detection threshold, the signal phase matched filter receiver gives superior performance.



Accession For	
NTIS GRA&I	<input checked="checked" type="checkbox"/>
DTIC TAB	<input type="checkbox"/>
Unannounced	<input type="checkbox"/>
Justification	
By	
Distribution/	
Availability Codes	
Dist	Avail and/or Special
A	

ABSTRACT

The signal detection characteristics of a two-input channel receiver are studied. The signals received on both channels are random Gaussian, narrowband processes identical except for a known channel-to-channel time delay. For narrowband representation, the time delay is treated as a differential phase modulation of the two signals. The noise on each of the two receiver channels is also random Gaussian processes which are jointly wide sense stationary and correlated. The receiver detects the presence of a signal by estimating the average phase difference between samples of the observed signals. The average phase is an input to a matched filter detector where the filter is matched to the known phase between the input signals. The receiver is intended to detect at signal-to-noise ratios less than 0 dB and over a wide range of noise correlation conditions.

The theoretical statistics required to predict the detection performance are developed. The receiver operating characteristic curves are generated from the likelihood functions at the matched filter output. An example of a possible signal phase function is considered and the receiver performance predicted.

The performance of the signal phase matched filter receiver is compared with a cross correlation receiver which includes a noise decorrelator and signal phase compensator. The cross correlation receiver is more sensitive than the signal phase matched filter receiver if the noise correlation is known. However, if the noise correlation is unknown

and the detection is made using fixed signal processing and detection threshold, the signal phase matched filter receiver gives superior performance.

TABLE OF CONTENTS

	<u>Page</u>
ABSTRACT	iii
LIST OF TABLES	vii
LIST OF FIGURES	viii
LIST OF SYMBOLS	x
ACKNOWLEDGEMENTS	xx
 <u>Chapter</u>	
I INTRODUCTION	1
1.1 Source of Detection Problem	1
1.2 Assumptions and Limitations	3
1.3 Background	4
1.4 Organization	5
II DETECTION PROBLEM	7
2.1 Signal and Noise Model	8
2.2 Sampling	15
2.3 Average Phase Estimate	18
2.4 Matched Filter Detector	21
III THEORETICAL DEVELOPMENT	26
3.1 Input Signal and Noise Characteristics	26
3.2 Statistical Properties of the Average Phase Estimate	29
3.2.1 Angle Average Phase Estimate	30
3.2.2 Vector Average Phase Estimate	32
3.3 Statistics of the Fourier Coefficients for Non-Stationary Periodic Input	42
3.3.1 Mean Value of Fourier Coefficient	45
3.3.2 Variance of Fourier Coefficient	45
3.3.3 Correlation of the Sine and Cosine Coefficients	48
3.3.4 Correlation Between Fourier Coefficients of Different Harmonics	48
3.3.5 Distribution of the Fourier Coefficients	50
3.4 Statistics of Threshold Detector Input	52
3.5 Receiver Operating Characteristics	54

TABLE OF CONTENTS (Con't)

<u>Chapter</u>	<u>Page</u>
IV DETECTION OF KNOWN SIGNALS	57
4.1 Linear Delay with Known Noise Correlation	58
4.2 Unknown Noise Correlation, Fixed Threshold Detector	68
4.3 Comparison with Cross Correlation Receiver	71
4.3.1 Known Noise Correlation	74
4.3.2 Unknown Noise Correlation	74
V SUMMARY AND CONCLUSIONS	79
5.1 Summary	79
5.2 Conclusions	80
5.3 Future Research	82
REFERENCES	83
APPENDIX A: SELECTED MIXED CENTRAL MOMENTS OF QUADRIVARIATE GAUSSIAN DENSITY FUNCTION	85
APPENDIX B: NOISE DECORRELATOR, SIGNAL PHASE COMPENSATION, CROSS CORRELATION RECEIVER	90

LIST OF TABLES

<u>Table</u>		<u>Page</u>
3-1	Moments for Fourier Coefficients of Non-Stationary Random Sequence	51
3-2	Approximate Value for Statistics of Fourier Coefficients Assuming Stationary Input Sequence	53

LIST OF FIGURES

<u>Figure</u>		<u>Page</u>
1-1	Moving Signal Source Detection Problem	2
2-1	Dual Channel Differential Phase Receiver	9
2-2	Signal-Noise Model	10
2-3	Quadrature Sampling of Observable Signals	16
2-4	Methods of Estimating Average Phase	19
2-5	Discrete Time Matched Filter Detector	25
3-1	Mean and Standard Deviation of Single Phase Estimate	31
3-2	Probability Density Function of Vector Average Phase Estimate	37
3-3	Mean and Standard Deviation of Vector Average Phase Estimate, $K_0 = 0.025$	38
3-4	Mean and Standard Deviation of Vector Average Phase Estimate, $K_0 = 0.10$	39
3-5	Mean and Standard Deviation of Vector Average Phase Estimate, $K_0 = 0.25$	40
3-6	Mean and Standard Deviation of Vector Average Phase Estimate, $K_0 = 0.50$	41
4-1	Approximate Matched Filter Configuration for Linear Delay	60
4-2	Variation in K_0 and ϕ_0 for Linear Delay and $SNR = -12$ dB	61
4-3	Mean and Variance of Angle Average Phase Estimate for Linear Delay and $SNR = -12$ dB	62
4-4	Mean and Variance of Vector Average Phase Estimate for Linear Delay and $SNR = -12$ dB	63
4-5	Detection Performance for Linear Delay and Angle Average Phase Estimate, Noise Correlation Known a Priori	65
4-6	Detection Performance for Linear Delay and Vector Correlation Known a Priori	66

<u>Figure</u>		<u>Page</u>
4-7	Detection Performance for Linear Delay, Angle Average Phase Estimate, Unknown Noise Correlation, and Threshold Set Assuming $K_N = 0.0$	69
4-8	Detection Performance for Linear Delay, Angle Average Phase Estimate, Unknown Noise Correlation, and Threshold Set Assuming $K_N = 0.5$, $\phi_N = 0$	70
4-9	Detection Performance for Linear Delay, Vector Average Phase Estimate, Unknown Noise Correlation, and Threshold Set Assuming $K_N = 0$	72
4-10	Detection Performance for Linear Delay, Vector Average Phase Estimate, Unknown Noise Correlation, and Threshold Set Assuming $K_N = 0.5$, $\phi_N = 0.0$	73
4-11	Detection Performance, Cross Correlation Receiver, Known Noise Correlation	75
4-12	Detection Performance, Cross Correlation Receiver, Unknown Noise Correlation and Threshold Set Assuming $K_N = 0$	77
4-13	Detection Performance, Cross Correlation Receiver, Unknown Noise Correlation and Threshold Set Assuming $K_N = 0.5$, $\phi_N = 0$	78
B-1	Cross Correlation Receiver	91

LIST OF SYMBOLS

$A_1(n)$	magnitude of $r_{p1}(n)$
$A_2(n)$	magnitude of $r_{p2}(n)$
$a_m(k)$	cosine Fourier coefficient of $\overline{\phi_a(m)}$
$a_s(k)$	cosine Fourier coefficient of $\phi_s(m)$
$a_v(k)$	cosine Fourier coefficient of $\sigma_a^2(m)$
$a_\phi(k)$	cosine Fourier coefficient of $\phi_a(m)$
$\overline{a_\phi(k)}$	mean value of $a_\phi(k)$
$b_m(k)$	sine Fourier coefficient of $\overline{\phi_a(m)}$
$b_s(k)$	sine Fourier coefficient of $\phi_s(m)$
$b_v(k)$	sine Fourier coefficient of $\sigma_a^2(m)$
$b_\phi(k)$	sine Fourier coefficient of $\phi_a(m)$
$\overline{b_\phi(k)}$	mean value of $b_\phi(k)$
$C(j\omega)$	characteristic function
$c_m(k)$	complex Fourier coefficient of $\overline{\phi_a(m)}$
$c_s(k)$	complex Fourier coefficient of $\phi_s(m)$
$c_v(k)$	complex Fourier coefficient of $\sigma_a^2(m)$
$c_\phi(k)$	complex Fourier coefficient of $\phi_a(m)$
$\overline{c_\phi(k)}$	mean value of $c_\phi(k)$
d	distance between sensors
dB	decibels
$E\{.\}$	expected value
$e(n)$	product of $r_{p1}(n)$ and $r_{p2}^*(n)$
G	gain
$H(k)$	transfer function, discrete frequency domain
$H(j\omega)$	transfer function, frequency domain

LIST OF SYMBOLS (Continued)

H_D	transfer function of noise decorrelator
H_m	transfer function of phase compensator
H_0	null hypothesis, no signal present
H_1	alternate hypothesis, signal present
h	signal-to-noise ratio
J	Jacobian
j	$\sqrt{-1}$
K_m	magnitude of phase compensation
$K_m(n)$	K_m as discrete time function
K_N	magnitude of noise correlation coefficient
\hat{K}_N	estimated value of K_N
K_o	magnitude of observable signal correlation coefficient
k	harmonic number
m	integer, sample number
m_x	mean value of X_a
m_y	mean value of y_a
N	number of points in processing interval
N_A	number of points averaged
N_F	number of points in DFT
n	integer, sampled time number
$n(t)$	input noise
$n_I(t)$	coherent noise
$n_{Ic}(t)$	in-phase component of $n_I(t)$
$n_{Is}(t)$	quadrature component of $n_I(t)$
$n_u(t)$	uncorrelate noise in channel 1

LIST OF SYMBOLS (Continued)

$n_{uc}(t)$	in-phase component of $n_u(t)$
$n_{us}(t)$	quadrature component of $n_u(t)$
$n_v(t)$	uncorrelated noise in channel 2
$n_{vc}(t)$	in-phase component of $n_v(t)$
$n_{vs}(t)$	quadrature component of $n_v(t)$
$n_1(t)$	input noise in channel 1
$n_{1c}(t)$	in-phase component of $n_1(t)$
$n_{1c}(n)$	discrete time $n_{1c}(t)$
$n_{1s}(t)$	quadrature component of $n_1(t)$
$n_{1s}(n)$	discrete time $n_{1s}(t)$
$n_2(t)$	input noise channel 2
$n_{2c}(t)$	in-phase component of $n_2(t)$
$n_{2c}(n)$	discrete time $n_{2c}(t)$
$n_{2s}(t)$	quadrature component of $n_2(t)$
$n_{2s}(n)$	discrete time $n_{2s}(t)$
P_D	probability of detection
\hat{P}_D	estimated P_D
$(P_D)_{aa}$	probability of detection, angle average phase estimate
$(P_D)_{va}$	probability of detection, vector average phase estimate
P_{fa}	probability of false alarm
$p(\underline{r})$	probability density function of \underline{r}
$p(r, \phi_{va})$	joint probability density function of r and ϕ_{va}
$p(\phi_{va})$	probability density function of ϕ_{va}
$p(\lambda_T)$	probability density function of λ_T
$p_o(\lambda_T)$	probability density function of λ_T given H_o
$p_1(\lambda_T)$	probability density function of λ_T given H_1

LIST OF SYMBOLS (Continued)

$p_{xy}(x,y)$	jointly probability density function of x_a and y_a
$p_1(n)$	output of noise decorrelator, channel 1
$p_2(n)$	output of noise decorrelator, channel 2
R	covariance matrix
R_r	covariance matrix of \underline{r}
R_p	covariance matrix of decorrelator output
R_u	covariance matrix of phase compensator output
\tilde{R}_u	isomorphic counterpart of R_u
ROC	receiver operating characteristics
r	amplitude of x_a and y_a
\underline{r}	$r_p(n)$ vector
$r(t)$	observable signal
$\hat{r}(t)$	Hilbert transform of $r(t)$
$r_c(t)$	in-phase component of $r(t)$
$r_c(n)$	in-phase component of $r_p(n)$
$r_p(n)$	discrete time $r(t)$
$r_{p1}(n)$	$r_p(n)$, channel 1
$r_{p2}(n)$	$r_p(n)$, channel 2
$r_s(n)$	quadrature component of $r_p(n)$
$r_1(t)$	$r(t)$, channel 1
$r_2(t)$	$r(t)$, channel 2
$r_{1c}(n)$	in-phase component of $r_{p1}(n)$
$r_{1s}(n)$	quadrature component of $r_{p1}(n)$
$r_{2c}(n)$	in-phase component of $r_{p2}(n)$
$r_{2s}(n)$	quadrature component of $r_{p2}(n)$

LIST OF SYMBOLS (Continued)

$s(j\omega)$	Fourier transform of $s(t)$
$s(k)$	discrete Fourier transform of $s(n)$
SNR	signal-to-noise ratio
$s(t)$	input signal
$s(n)$	discrete time $s(t)$
$s_c(t)$	in-phase component of $s(t)$
$s_c(n)$	discrete time $s_c(t)$
$s_s(t)$	quadrature component of $s(t)$
$s_s(n)$	discrete time $s_s(n)$
T	period of $s(t)$
t	time
u	complex variable
\underline{u}	state vector, phase compensator output
u_c	real component of u
u_s	imaginary component of u
$u_1(n)$	phase compensator output, channel 1
$u_2(n)$	phase compensator output, channel 2
v	complex variable
\underline{v}	velocity vector
v_c	real part of v
v_s	imaginary part of v
$x(n)$	real part of $e(n)$
\bar{x}	mean value of $x(n)$
x_a	average value of $x(n)$
\bar{x}_a	mean value of x_c

LIST OF SYMBOLS (Continued)

$y(n)$	imaginary part of $e(n)$
\bar{y}	mean value of $y(n)$
y_a	average value of $y(n)$
\bar{y}_a	mean value of y_a
\underline{z}	vector
z_1	component of \underline{z}
z_2	component of \underline{z}
z_3	component of \underline{z}
z_4	component of \underline{z}
$\alpha(r, \phi_{va})$	function of r and ϕ_{va}
α_u^2	component of \vec{R}_u
β	variable
δ	non-centrality factor
$\epsilon(K_o)$	function of K_o
$\lambda(\lambda_T)$	likelihood ratio
λ_{aa}	λ_T , angle average phase estimate
$\bar{\lambda}_{aa}$	mean value of λ_{aa}
$\bar{\lambda}_c$	correlation receiver test statistic
λ_N	imaginary part of noise correlation coefficient
λ_T	test statistic
$\bar{\lambda}_T$	mean value of λ_T
$\hat{\lambda}_T$	estimated λ_T
λ_{TH}	threshold setting
λ_{To}	λ_T given H_o

LIST OF SYMBOLS (Continued)

$\bar{\lambda}_{To}$	mean value of λ_{To}
λ_{T1}	λ_T given H_1
$\bar{\lambda}_{T1}$	mean value of λ_{T1}
λ_u	component of \vec{R}_u
λ_{va}	λ_{va} , vector average phase estimate
$\bar{\lambda}_{va}$	mean value of λ_{va}
λ_1	output of correlator
λ_2	output of power estimator
μ_a	covariance, x_a and y_a
$\mu_a(k, \ell)$	covariance, $a_s(k)$ and $a_s(\ell)$
$\mu_{ab}(k)$	covariance, $a_s(k)$ and $b_s(k)$
$\mu_{ab}(k, \ell)$	covariance, $a_s(k)$ and $b_s(\ell)$
$\mu_b(k, \ell)$	covariance, $b_s(k)$ and $b_s(\ell)$
$\mu_c(k, \ell)$	covariance, $c_s(k)$ and $c_s(\ell)$
μ_{xy}	covariance, $x(n)$ and $y(n)$
μ_x	covariance between λ_1 and λ_2
$\mu_{1c, 2c}$	covariance, $n_{1c}(t)$ and $n_{2c}(t)$
$\mu_{1c, 2s}$	covariance, $n_{1c}(t)$ and $n_{2s}(t)$
$\mu_{1s, 2c}$	covariance, $n_{1s}(t)$ and $n_{2c}(t)$
$\mu_{1s, 2s}$	covariance, $n_{1s}(t)$ and $n_{2s}(t)$
π	mathematic constant, 3.14159265
ρ_N	real part of noise correlation coefficient
ρ_u	component of \vec{R}_u
ρ_{xy}	correlation between x_a and y_a
$\sigma_a^2(k)$	variance of $a_s(k)$
$\sigma_{aa}^2(k)$	variance of ϕ_{aa}

LIST OF SYMBOLS (Continued)

$\sigma_b^2(k)$	variance of $b_s(k)$
$\sigma_c^2(k)$	variance of $c_s(k)$
$\sigma_I^2(k)$	variance of $n_I(t)$
σ_n^2	variance of $n(t)$
σ_o^2	variance of $r(t)$
σ_s^2	variance of $s(t)$
σ_u^2	variance of $n_u(t)$
σ_v^2	variance of $n_v(t)$
σ_{va}^2	variance of ϕ_{va}
σ_x^2	variance of $x(n)$
σ_{xa}^2	variance of x_a
σ_y^2	variance of $y(n)$
σ_{ya}^2	variance of $y_a(n)$
σ_1^2	variance of λ_1
σ_2^2	variance of λ_2
σ_λ^2	variance of λ_T
$\hat{\alpha}_\lambda^2$	estimate of α_λ^2
$\alpha_{\lambda o}^2$	α_λ^2 given H_o
$\alpha_{\lambda 1}^2$	α_λ^2 given H_1
$(\alpha_\lambda^2)_{aa}$	α_λ^2 , angle average phase estimate
$(\alpha_\lambda^2)_{va}$	α_λ^2 , vector average phase estimate
σ_ϕ^2	variance of ϕ
$\sigma_{\phi a}^2$	variance of ϕ_a
τ_N	time delay for $N_I(t)$
$\tau_s(t)$	varying time delay for $s(t)$

LIST OF SYMBOLS (Continued)

ϕ	phase difference between $r_{p1}(n)$ and $r_{p2}(n)$
$\bar{\phi}$	mean value of ϕ
$\bar{\phi}(n)$	discrete time ϕ
ϕ_a	average phase
$\phi_a(m)$	discrete time ϕ_a
$\bar{\phi}_a$	mean value of ϕ_a
ϕ_{aa}	angle average phase
$\phi_{aa}(m)$	discrete time ϕ_{aa}
$\bar{\phi}_{aa}$	mean value of ϕ_{aa}
ϕ_I	phase associated by τ_N
ϕ_m	phase of phase compensator
$\phi_m(n)$	discrete time ϕ_m
ϕ_N	phase of noise correlation coefficient
$\phi_N(n)$	discrete time ϕ_N
$\hat{\phi}_N$	estimate of ϕ_N
ϕ_o	phase of observable signal correlation coefficient
ϕ_p	peak value of $\phi_s(t)$
ϕ_s	signal phase
$\phi_s(t)$	time function of ϕ_s
$\phi_s(n)$	discrete time ϕ_s
ϕ_{va}	vector average phase
$\bar{\phi}_{va}$	mean value of ϕ_{va}
$\phi_{va}(n)$	discrete time ϕ_{va}
$\phi_1(n)$	phase of $r_{p1}(n)$
$\phi_2(n)$	phase of $r_{p2}(n)$
$\underline{\omega}$	vector

LIST OF SYMBOLS (Concluded)

ω_c	center frequency of narrowband input processes
ω_1	component of $\underline{\omega}$
ω_2	component of $\underline{\omega}$
ω_3	component of $\underline{\omega}$
ω_4	component of $\underline{\omega}$

ACKNOWLEDGEMENTS

This research was supported by the Applied Research Laboratory of The Pennsylvania State University under contract with the Naval Sea Systems Command.

CHAPTER I

INTRODUCTION

1.1 Source of Detection Problem

Radiation from a moving source produces a varying time delay between signals received by two sensors which are separated by a baseline. If the geometry of the moving source and the sensors is known, the varying time delay can be predicted prior to detection of the signals. A receiver which uses this known, varying time delay as a basis to detect the presence of a signal source moving on a known course through a field of stationary interfering noise sources has been investigated and its detection characteristics have been defined.

Figure 1-1 shows a signal source which is passing with a known motion through a field of stationary noise sources. The moving source radiates a Gaussian signal which is received by two physically separated, narrow-band sensors. The time delay between the Gaussian, narrowband signals at the sensor outputs is determined by the source motion and the relative geometry of the source and sensors. The time delay is treated as a phase delay in expressing the received, narrowband signals.

The presence of stationary interference noise sources in an isotropic Gaussian background noise field results in an anisotropic noise field. This anisotropic noise combines with the electrical noise of the sensors such that the noise at the filtered sensor outputs is correlated. The sensor output noise is stationary and Gaussian with unknown power level.

This research studied the detection problem after the reception of the signals and noise by the two sensors. The problem investigated is

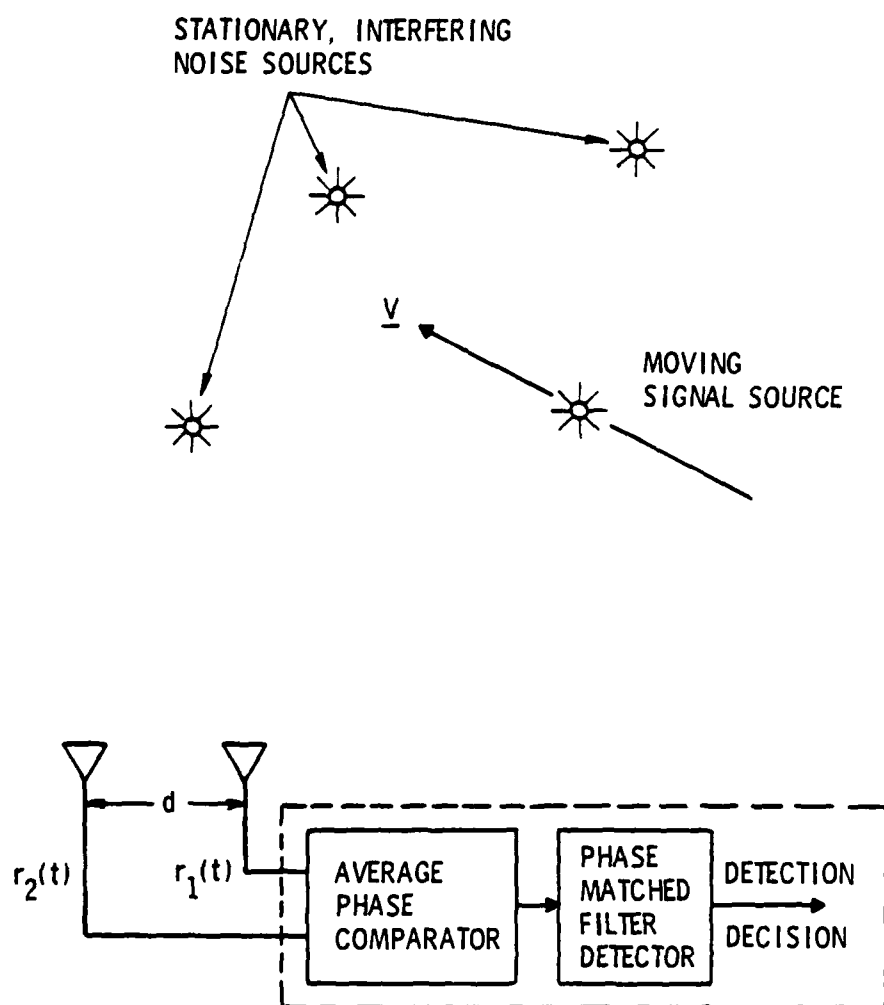


FIGURE 1-1. Moving Signal Source Detection Problem.

the signal detection characteristics of a receiver with two input channels. The signals in both channels are narrowband, random, Gaussian processes which are identical except for a known, time varying phase delay. The input noise is correlated, Gaussian noise of unknown power level. The receiver detection process estimates the average phase difference between the observed signals in the two receiver input channels. The estimated average phase is an input to a detector which is an approximation of a matched filter detector for the known phase delay between the desired input signals.

1.2 Assumptions and Limitations

The signal detection system is intended to function at low signal-to-noise ratios and over a variety of noise correlation values. The signal processing is to be implemented using digital techniques. These factors and the nature of the original detection problem result in a number of assumptions. Any limitations imposed by these assumptions must be considered when interpreting the results.

The received signal is a stationary narrowband, zero-mean Gaussian stochastic process. The signal in one input is a phase-shifted version of the signal in the other input. The signal power level is equal in each input. The time varying phase delay between the input signals is known. The bandwidth of the input signals is much greater than the bandwidth associated with the time varying phase delay.

The noise in the two inputs is jointly stationary, correlated, zero-mean, narrowband Gaussian noise. The power level of the noise is unknown, but it is the same in each input. The detection process is investigated for both known and unknown noise correlation cases.

The system is intended to detect at signal-to-noise ratios less than 0 dB. The signal-processing interval is selected to be long enough to achieve this goal.

The inputs are sampled and digitized. It is assumed that the sampling period is adjusted to the input bandwidth such that sequential samples are statistically independent.

1.3 Background

Detection of a Gaussian signal in Gaussian noise has been widely investigated in the past [1], [2], [3]. The likelihood detector is commonly used to detect signals which are not completely known. If the input noise is correlated, the likelihood detector can be implemented using a noise de-correlator or spatial prewhitener [4]. These investigations assumed the noise power level and noise correlation were known. If the power level is unknown, a detector can be implemented consisting of two channels [5], [6]. One channel has the form of a likelihood ratio detector and the other channel is a minimum variance power level estimator. With two inputs, this detector takes the form of a cross correlation detector. Source motion causes degradation in the output of the correlator, unless the correlator implements a compensation delay modulation, [7], [8].

Based on the above background, a receiver which could be used to solve the detection problem would consist of a noise decorrelator, time delay compensation modulator and cross correlation detector. Such a receiver requires that the noise correlation be known in order to obtain maximum sensitivity.

An alternative to the classical likelihood detector is a receiver which estimates the phase between the signals at the filtered sensor outputs. The signal is then detected using a matched filter detector [9]. The filter is matched to the known phase delay. This alternate receiver is analyzed and its detection characteristics determined.

1.4 Organization

Chapter II contains a detailed description of the detection problem. The generalized received signal and noise model is explained. This is followed by a description of the methods of estimating phase difference and a description of the matched filter detector.

The theoretical statistics required to determine the detection system performance are developed in Chapter III. These statistics are a function of the input signal-to-noise ratio and the correlation characteristics of the noise in the two channels of the receiver. Major emphasis is placed on the statistics of the average phase estimate. The material in this chapter forms the theoretical basis for understanding the signal detection problem.

In Chapter IV, the receiver detection characteristics are determined for a linear phase delay function. The matched filter configuration is described, the effect of phase averaging examined and the theoretical detection curves generated. The above assumes the noise correlation is known. The chapter ends by investigating detection performance for the unknown noise correlation case.

A performance comparison with the cross correlation detector is made. This performance comparison is made for both known noise

correlation and unknown noise correlation cases. The cross correlation detector with noise de-correlator and phase shift compensation is described in Appendix B.

Conclusions and recommendations are contained in Chapter V.

CHAPTER II

DETECTION PROBLEM

Detecting a dual channel differential phase modulated signal in the presence of correlated noise is a problem in selecting one of two possible hypotheses, the desired signal is present or the desired signal is not present. The receiver being studied uses the Neyman-Pearson criterion [10] to test the hypotheses. This criterion maximizes the probability of detection for a given probability of false alarm. The observable signals at the receiver inputs may be of two forms:

$$r_1(t) = \left\{ \begin{array}{c} 0 \\ \text{or} \\ s(t) \end{array} \right\} + n_1(t)$$

$$r_2(t) = \left\{ \begin{array}{c} 0 \\ \text{or} \\ s[t - \tau(t)] \end{array} \right\} + n_2(t)$$

where $r(t)$ = observable signal

$s(t)$ = desired signal

$n(t)$ = noise

$\tau(t)$ = time delay.

The receiver is designed to operate on the observable signals and select either the null hypothesis, H_0 , or the alternative hypothesis, H_1 .

Symbolically these hypotheses are:

$$H_0: \left\{ \begin{array}{ll} r_1(t) = n_1(t) & , 0 \leq t \leq T \\ r_2(t) = n_2(t) & , 0 \leq t \leq T \end{array} \right\} \quad (2-1)$$

$$H_1: \left\{ \begin{array}{ll} r_1(t) = s(t) + n_1(t) & , 0 \leq t \leq T \\ r_2(t) = s[t - \tau_s(t)] + n_2(t) & , 0 \leq t \leq T \end{array} \right\} \quad (2-2)$$

where T = period of $s(t)$.

Figure 2-1 shows a block diagram of the receiver being studied. The receiver consists of four basic blocks. The observed signals are sampled and digitized. An estimate is made of the average difference between phases of the two observable sequences. The resulting average phase sequence is an input to a matched filter. The transfer function of the filter is matched to the differential phase shift between the desired signals received in the two input channels. If the filter output exceeds a threshold, the H_1 hypothesis, signal present, is selected. If the threshold is not exceeded, the H_0 hypothesis, no signal present, is selected.

2.1 Signal and Noise Model

The signal-noise model for the generalized detection problem is shown in Figure 2-2. The noise sources $n_u(t)$, $n_v(t)$ and $n_l(t)$ are always present. The signal $s(t)$, which may or may not be present, is a random narrowband Gaussian process with zero mean. A random process is narrowband if its spectral density is zero except for a narrow region around a high carrier frequency [11]. The received signal can be expressed as:

$$s(t) = s_c(t) \cos \omega_c t - s_s(t) \sin \omega_c t \quad (2-3)$$

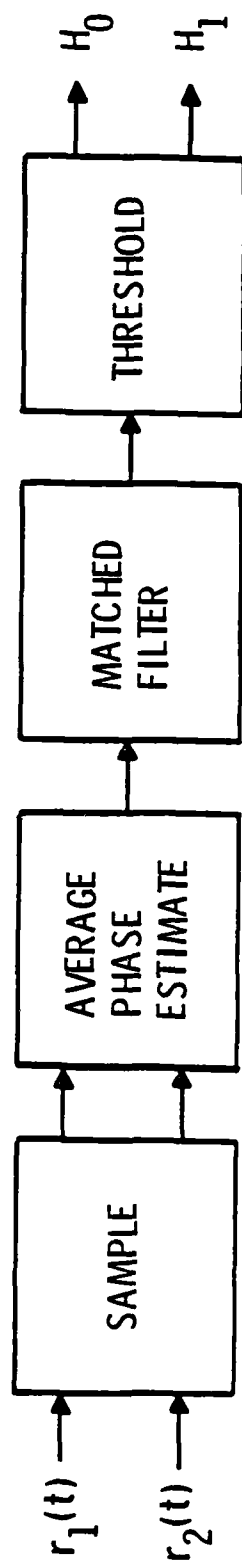


FIGURE 2-1. Dual Channel Differential Phase Receiver.

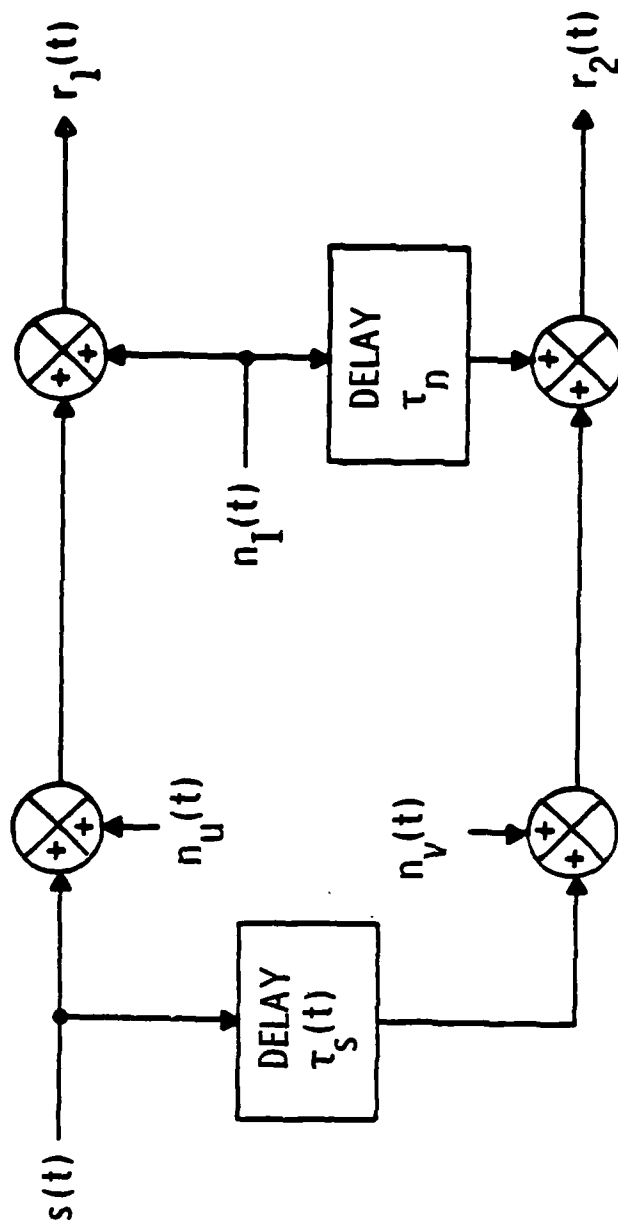


FIGURE 2-2. Signal-Noise Model.

where $s_c(t)$ = the in-phase component of $s(t)$
 $s_s(t)$ = the quadrature component of $s(t)$
 ω_c = the center frequency of the narrowband spectral
density of $s(t)$.

It is assumed that the maximum rate with which the time delay, $\tau_s(t)$, varies is very small when compared to the inverse of the signal bandwidth. The signal bandwidth is defined by the receiver passband. The in-phase and quadrature components of the time-delayed signal can therefore be considered to be:

$$\begin{aligned} s_c[t - \tau_s(t)] &\approx s_c(t) \\ s_s[t - \tau_s(t)] &\approx s_s(t). \end{aligned}$$

The time-delayed signal is approximated as:

$$s[t - \tau_s(t)] \approx s_c(t) \cos [\omega_c t - \omega_c \tau_s(t)] - s_s(t) \sin [\omega_c t - \omega_c \tau_s(t)].$$

If the $\omega_c \tau_s(t)$ is considered to be a variable phase,

$$\phi_s(t) = \omega_c \tau_s(t),$$

the time delayed signal may be expressed as:

$$s[t - \tau_s(t)] = s_c(t) \cos [\omega_c t - \phi_s(t)] - s_s(t) \sin [\omega_c t - \phi_s(t)]. \quad (2-4)$$

The signals in the two channels of the receiver are expressed as:

$$\left. \begin{aligned} s_1(t) &= s_c(t) \cos \omega_c t - s_s(t) \sin \omega_c t \\ s_2(t) &= s_c(t) \cos [\omega_c t - \phi_s(t)] - s_s(t) \sin [\omega_c t - \phi_s(t)]. \end{aligned} \right\} \quad (2-5)$$

The total received noise is the sum of the contributions from the receiver electrical noise, the isotropic noise field and all stationary interference sources. The received noise is represented by three independent noise sources in the signal-noise model. The noise in each channel can be considered to be the sum of a common or fully correlated component and an independent component. The independent components are represented by $n_u(t)$ and $n_v(t)$. The common component is $n_I(t)$. The fixed time delay τ_n associated with $n_I(t)$ is a composite of the time delays of all the interference sources.

As these noise sources are independent random narrowband processes, they can be expressed:

$$\left. \begin{aligned} n_u(t) &= n_{uc}(t) \cos \omega_c t - n_{us}(t) \sin \omega_c t \\ n_v(t) &= n_{vc}(t) \cos \omega_c t - n_{vs}(t) \sin \omega_c t \\ n_I(t) &= n_{Ic}(t) \cos \omega_c t - n_{Is}(t) \sin \omega_c t \\ n_I(t-\tau_n) &= n_{Ic}(t) \cos (\omega_c t - \phi_I) - n_{Is}(t) \sin (\omega_c t - \phi_I) \end{aligned} \right\} \quad (2-6)$$

where

$$\phi_I = \omega_c \tau_n .$$

Using the above narrowband representation, the noise in the two receiver channels is:

$$\left. \begin{aligned} n_1(t) &= [n_{uc}(t) + n_{Ic}(t)] \cos \omega_c t - [n_{us}(t) + n_{Is}(t)] \sin \omega_c t \\ n_2(t) &= [n_{vc}(t) + n_{Ic}(t) \cos \phi_I + n_{Is}(t) \sin \phi_I] \cos \omega_c t \\ &\quad - [n_{vs}(t) - n_{Ic}(t) \sin \phi_I + n_{Is}(t) \cos \phi_I] \sin \omega_c t . \end{aligned} \right\} \quad (2-7)$$

The in-phase and quadrature components of $n_1(t)$ and $n_2(t)$ are:

$$\left. \begin{aligned} n_{1c}(t) &= n_{uc}(t) + n_{Ic}(t) \\ n_{1s}(t) &= n_{us}(t) + n_{Is}(t) \\ n_{2c}(t) &= n_{vc}(t) + n_{Ic}(t) \cos \phi_I + n_{Is}(t) \sin \phi_I \\ n_{2s}(t) &= n_{vs}(t) - n_{Ic}(t) \sin \phi_I + n_{Is}(t) \cos \phi_I \end{aligned} \right\} \quad (2-8)$$

The mean, variance and covariance of the in-phase and quadrature components of the noise are important parameters in determining the detection statistics. It is assumed that the receiver is designed such that the power level of the noise in each channel is equal.

$$\sigma_u^2 = \sigma_v^2 \quad (2-9)$$

Since the noise sources are all assumed to be zero mean processes, the mean values of the noise components are:

$$E\{n_{1c}(t)\} = E\{n_{1s}(t)\} = E\{n_{2c}(t)\} = E\{n_{2s}(t)\} = 0 ; \quad (2-10)$$

the variances are:

$$\left. \begin{aligned} E\{n_{1c}^2(t)\} &= \sigma_u^2 + \sigma_I^2 = \sigma_N^2 \\ E\{n_{1s}^2(t)\} &= \sigma_u^2 + \sigma_I^2 = \sigma_N^2 \\ E\{n_{2c}^2(t)\} &= \sigma_v^2 + \sigma_I^2 (\cos^2 \phi_I + \sin^2 \phi_I) = \sigma_N^2 \\ E\{n_{2s}^2(t)\} &= \sigma_v^2 + \sigma_I^2 (\sin^2 \phi_I + \cos^2 \phi_I) = \sigma_N^2 \end{aligned} \right\} \quad (2-11)$$

where

$$\sigma_u^2 \triangleq E\{n_u^2(t)\}$$

$$\sigma_v^2 \triangleq E\{n_v^2(t)\}$$

$$\sigma_I^2 \triangleq E\{n_I^2(t)\}$$

and the covariances between components are:

$$E\{n_{1c}(t) n_{1s}(t)\} = E\{n_{2c}(t) n_{2s}(t)\} = 0$$

$$E\{n_{1c}(t) n_{2c}(t)\} \triangleq \mu_{1c,2c} = \sigma_I^2 \cos \phi_I$$

$$E\{n_{1c}(t) n_{2s}(t)\} \triangleq \mu_{1c,2s} = -\sigma_I^2 \sin \phi_I$$

$$E\{n_{1s}(t) n_{2c}(t)\} \triangleq \mu_{1s,2c} = \sigma_I^2 \sin \phi_I$$

$$E\{n_{1s}(t) n_{2s}(t)\} \triangleq \mu_{1s,2s} = \sigma_I^2 \cos \phi_I$$

(2-12)

When one defines

$$\rho_N \triangleq \frac{\sigma_I^2}{\sigma_N^2} \cos \phi_I$$

$$\lambda_N \triangleq \frac{\sigma_I^2}{\sigma_N^2} \sin \phi_I$$

$$K_N^2 \triangleq \rho_N^2 + \lambda_N^2 = \frac{\sigma_I^2}{\sigma_N^2}$$

$$\phi_N \triangleq \tan^{-1} \left(\frac{\lambda_N}{\rho_N} \right) = \phi_I$$

(2-13)

the covariances become

$$\left. \begin{aligned} \mu_{1c,1s} &= \mu_{2c,2s} = 0 \\ \mu_{1c,2c} &= \mu_{1s,2s} = \rho_N \sigma_N^2 = \sigma_N^2 K_N \cos \phi_N \\ -\mu_{1c,2s} &= \mu_{1s,2c} = \lambda_N \sigma_N^2 = \sigma_N^2 K_N \cos \phi_N \end{aligned} \right\} \quad (2-14)$$

Thus, the noise in the two channels of the receiver is correlated.

The observable signals are the sum of equations (2-5) and (2-7). Using the noise components defined by equations (2-8), the observable signals become:

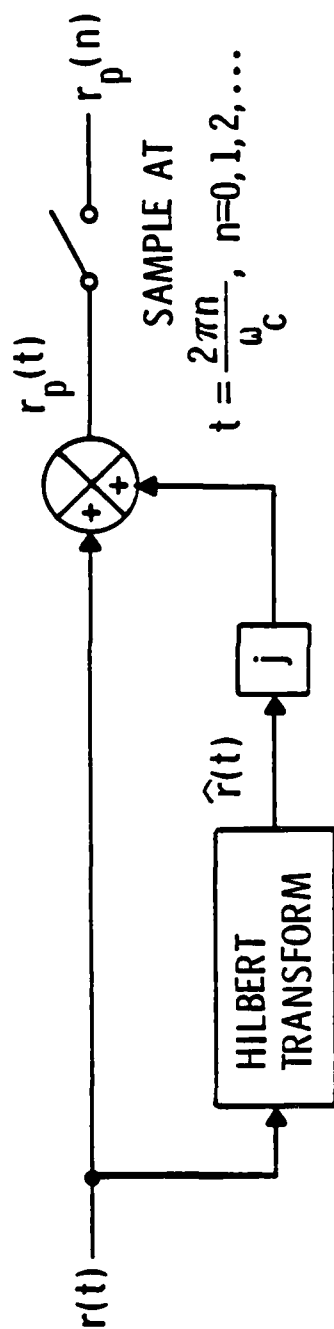
$$\left. \begin{aligned} r_1(t) &= [s_c(t) + n_{1c}(t)] \cos \omega_c t - [s_s(t) + n_{1s}(t)] \sin \omega_c t \\ r_2(t) &= [s_c(t) \cos \phi_s(t) + s_s(t) \sin \phi_s(t) + n_{2c}(t)] \cos \omega_c t \\ &\quad - [-s_c(t) \sin \phi_s(t) + s_s(t) \cos \phi_s(t) + n_{2s}(t)] \sin \omega_c t \end{aligned} \right\} \quad (2-15)$$

2.2 Sampling

The observable signals $r_1(t)$ and $r_2(t)$ are quadrature sampled. Quadrature sampling of a narrowband signal is equivalent to sampling of the analytic signal or pre-envelope [12]. Quadrature sampling is shown in Figure 2-3. The analytic signal $r_p(t)$ is formed by the complex function

$$r_p(t) = r(t) + j \hat{r}(t)$$

where $\hat{r}(t)$ is the Hilbert Transform of $r(t)$. For a narrowband signal



$$r(t) = r_c(t) \cos \omega_c t - r_s(t) \sin \omega_c t, \quad r_p(n) = r_c(n) + j r_s(n)$$

FIGURE 2-3. Quadrature Sampling of Observable Signals.

$r(t)$ the analytic signal is:

$$r_p(t) = [r_c(t) + j r_s(t)] e^{j\omega_c t}$$

The analytic signal is sampled to obtain the complex low pass signal

$r_c(t) + j r_s(t)$. Thus, the sampled signal is:

$$r_p(n) = r_c(n) + j r_s(n)$$

The sampling is at a rate which is equal to or greater than the inverse of the bandwidth of the low pass signal [13].

After quadrature sampling, the observable signals can be expressed as:

$$\left. \begin{aligned} r_{p1}(n) &= [s_c(n) + n_{1c}(n)] + j[s_s(n) + n_{1s}(n)] \\ r_{p2}(n) &= [s_c(n) \cos \phi_s(n) + s_s(n) \sin \phi_s(n) + n_{2c}(n)] \\ &\quad + j[-s_c(n) \sin \phi_s(n) + s_s(n) \cos \phi_s(n) + n_{2s}(n)] \end{aligned} \right\} \quad (2-16)$$

The complex sequences $r_{p1}(n)$ and $r_{p2}(n)$ may be expressed in terms of their amplitude and phase,

$$r_{p1}(n) = A_1(n) e^{j\phi_1(n)} \quad (2-17)$$

where

$$A_1(n) = \{ [s_c(n) + n_{1c}(n)]^2 + [s_s(n) + n_{1s}(n)]^2 \}^{1/2}$$

$$\phi_1(n) = \tan^{-1} \left[\frac{s_s(n) + n_{1s}(n)}{s_c(n) + n_{1c}(n)} \right]$$

and

$$r_{p2}(n) = A_2(n) e^{j\phi_2(n)} \quad (2-18)$$

where

$$A_2(n) = \left\{ \left[s_c(n) \cos \phi_s(n) + s_s(n) \sin \phi_s(n) + n_{2c}(n) \right]^2 + \left[-s_c(n) \sin \phi_s(n) + s_c(n) \cos \phi_s(n) + n_{2s}(n) \right]^2 \right\}^{1/2}$$

$$\phi_2(n) = \tan^{-1} \left[\frac{-s_c(n) \sin \phi_s(n) + s_c(n) \cos \phi_s(n) + n_{2s}(n)}{s_c(n) \cos \phi_s(n) + s_s(n) \sin \phi_s(n) + n_{2c}(n)} \right]$$

2.3 Average Phase Estimate

It has been noted that the bandwidth of the received signal is assumed to be much greater than the bandwidth of the time delay function. Therefore, processing of the estimated phase difference between $r_{p1}(n)$ and $r_{p2}(n)$ may be simplified by averaging. Two methods that can be used to make an average phase estimate are shown in Figure 2-4. These two methods are identified as angle average and vector average.

If the complex conjugate of $r_{p2}(n)$ is multiplied by $r_{p1}(n)$ the product will be:

$$e(n) = r_{p1}(n) r_{p2}^*(n)$$

$$= A_1(n) A_2(n) e^{j[\phi_1(n) - \phi_2(n)]}$$
(2-19)

Thus, the phase of $e(n)$ is the phase difference of sequences $r_{p1}(n)$ and $r_{p2}(n)$. Assuming that no noise is present, the signal phase in each of

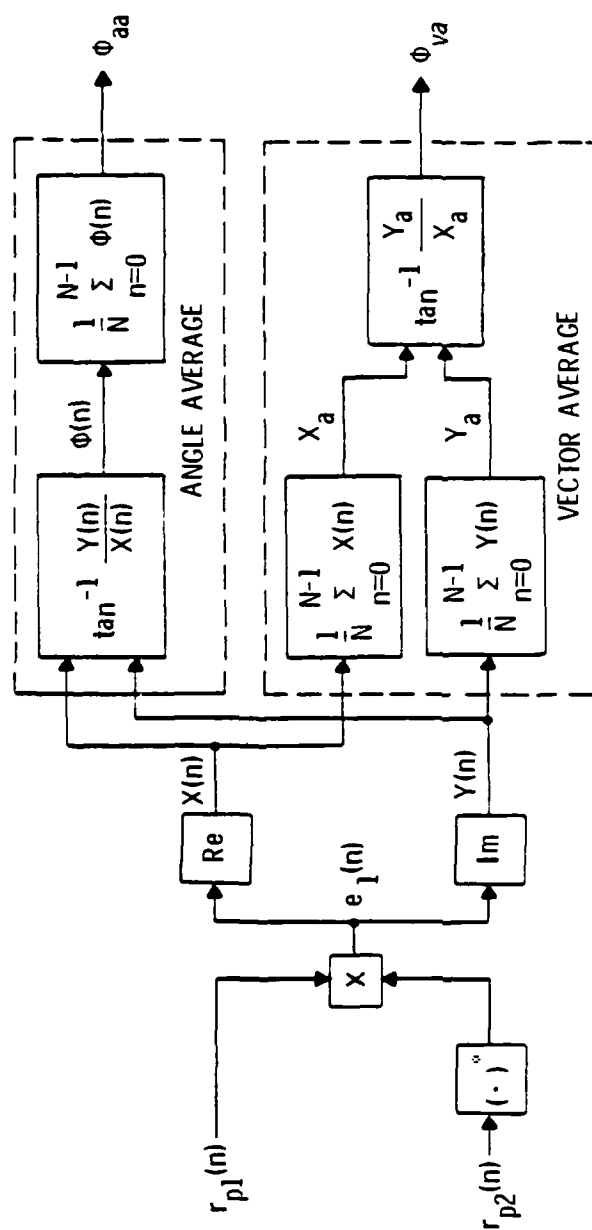


FIGURE 2-4. Methods of Estimating Average Phase.

the receiver channels is:

$$\begin{aligned}\phi_1(n) &= \tan^{-1} \left[\frac{s_s(n)}{s_c(n)} \right] \\ \phi_2(n) &= \tan^{-1} \left[\frac{s_s(n) \cos \phi_s(n) - s_c(n) \sin \phi_s(n)}{s_c(n) \cos \phi_s(n) + s_s(n) \sin \phi_s(n)} \right] \\ &= \tan^{-1} \left\{ \frac{\left[\frac{s_s(n)}{s_c(n)} \right] - \left[\frac{\sin \phi_s(n)}{\cos \phi_s(n)} \right]}{1 + \left[\frac{s_s(n)}{s_c(n)} \right] \left[\frac{\sin \phi_s(n)}{\cos \phi_s(n)} \right]} \right\} .\end{aligned}\tag{2-20}$$

Since

$$\tan(\alpha - \beta) = \frac{\tan \alpha - \tan \beta}{1 + \tan \alpha \tan \beta} ,$$

the phase in channel 2 is

$$\phi_2(n) = \phi_1(n) - \phi_s(n) .\tag{2-21}$$

The phase difference is then

$$\phi_1(n) - \phi_2(n) = \phi_s(n) .\tag{2-22}$$

The phase of $e(n)$ is the difference between the phase of the signals in the two receiver channels. When noise is added to the observable signal, the assumption that the phase of $e(n)$ is the desired signal phase difference is no longer certain.

To estimate the average phase of the complex sequence $e(n)$, the sequence is first divided into its real and imaginary components. If

$$e(n) = |e(n)| e^{j\phi_N(n)} ,$$

then

$$X(n) \triangleq \text{Re} [e(n)] = |e(n)| \cos \phi_N(n) \quad (2-23)$$

$$Y(n) \triangleq \text{Im} [e(n)] = |e(n)| \sin \phi_N(n) . \quad (2-24)$$

To obtain the angle average phase, ϕ_{aa} , the phase of the individual samples is calculated and then averaged.

$$\phi_{aa} = \frac{1}{N_a} \sum_{n=0}^{N_a-1} \tan^{-1} \left(\frac{Y(n)}{X(n)} \right) . \quad (2-25)$$

The vector average phase is calculated by first averaging the real and imaginary components and then calculating a phase from these average vector components

$$\phi_{va} = \tan^{-1} \left[\frac{\sum_{n=0}^{N_a-1} Y(n)}{\sum_{n=0}^{N_a-1} X(n)} \right] \quad (2-26)$$

The average phase statistics will be studied in Chapter III.

2.4 Matched Filter Detector

The matched filter transfer function is defined to be:

$$H(j\omega) = S^*(j\omega) e^{-j\omega T} \quad (2-27)$$

where $S(j\omega)$ = the Fourier transform of the desired signal

T = processing interval.

If the signal has a period T and is sampled and expanded in a Discrete Fourier Series [14], the digital equivalent to the matched filter

transfer function is:

$$H(k) = S^*(k) \quad (2-28)$$

where $H(k)$ = impulse response or transfer function of discrete
time matched filter

$S(k)$ = coefficients of discrete Fourier series representation
of $S(m)$.

The input to the matched filter is the average phase sequence $\phi_a(m)$. For the desired signal, the phase sequence $\phi_a(m)$ would be the signal phase $\phi_s(m)$ corresponding to the known time delay $\tau_s(t)$. Therefore, the frequency response of the desired signal is:

$$C_s(k) = \sum_{m=0}^{N_F-1} \phi_s(m) e^{-j \frac{2\pi km}{N_F}}, \quad 0 \leq k \leq N_F-1 \quad (2-29)$$

where N_F = period of Discrete Fourier Series.

The Fourier coefficients of input to the matched filter are:

$$C_\phi(k) = \sum_{m=0}^{N_F-1} \phi_a(m) e^{-j \frac{2\pi km}{N_F}}, \quad 0 \leq k \leq N_F-1 \quad (2-30)$$

The Fourier transforms can also be expressed in terms of the sine and cosine components.

$$C_s(k) = a_s(k) + j b_s(k)$$

$$C_\phi(k) = a_\phi(k) + j b_\phi(k) \quad .$$

The output of the matched filter, λ_T , is

$$\lambda_T = \frac{1}{N_F} \sum_{k=0}^{N_F-1} C_\phi(k) C_s^*(k) \quad (2-31)$$

Expressing equation (2-31) using the sine and cosine Fourier components

$$\begin{aligned}\lambda_T &= a_\phi(0) a_s(0) + \frac{1}{N} \sum_{k=1}^{N_F-1} [a_\phi(k) + j b_\phi(k)] [a_s(k) - j b_s(k)] \\ \lambda_T &= a_\phi(0) a_s(0) + \frac{1}{N} \sum_{k=1}^{N_F-1} [a_\phi(k) a_s(k) + b_\phi(k) b_s(k)] \\ &\quad - \frac{1}{N_F} \sum_{k=1}^{N_F-1} [a_s(k) b_\phi(k) - a_\phi(k) b_s(k)] .\end{aligned}$$

For a real sequence, the cosine terms are even functions and the sine terms are odd functions

$$a(k) = a(n-k)$$

$$b(k) = -b(n-k)$$

Therefore, the output of the matched filter can be expressed as

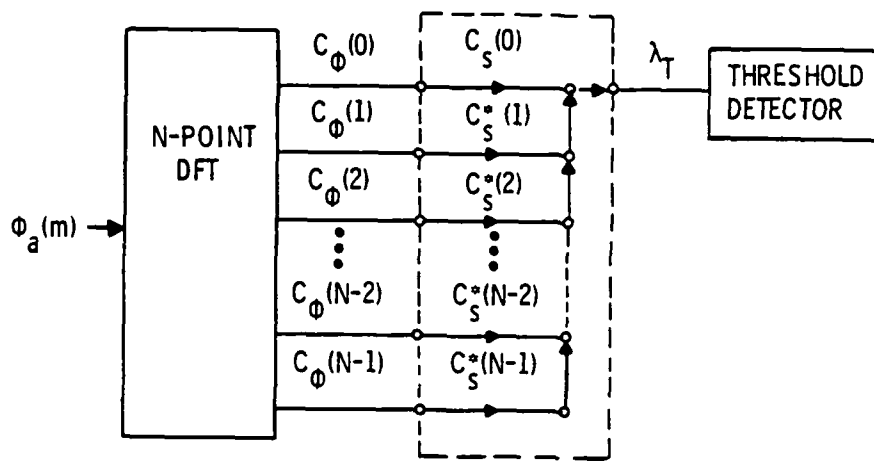
$$\begin{aligned}\lambda_T &= a_\phi(0) a_s(0) + \frac{2}{N_F} \sum_{k=1}^{\frac{N_F}{2}-1} [a_\phi(k) a_s(k) + b_\phi(k) b_s(k)] \\ &\quad + a_\phi\left(\frac{N_F}{2}\right) a_s\left(\frac{N_F}{2}\right) , \quad N \text{ even}\end{aligned}$$

If the $a_s(0)$ and $a_s\left(\frac{N}{2}\right)$ terms equal zero, the output of the matched filter is

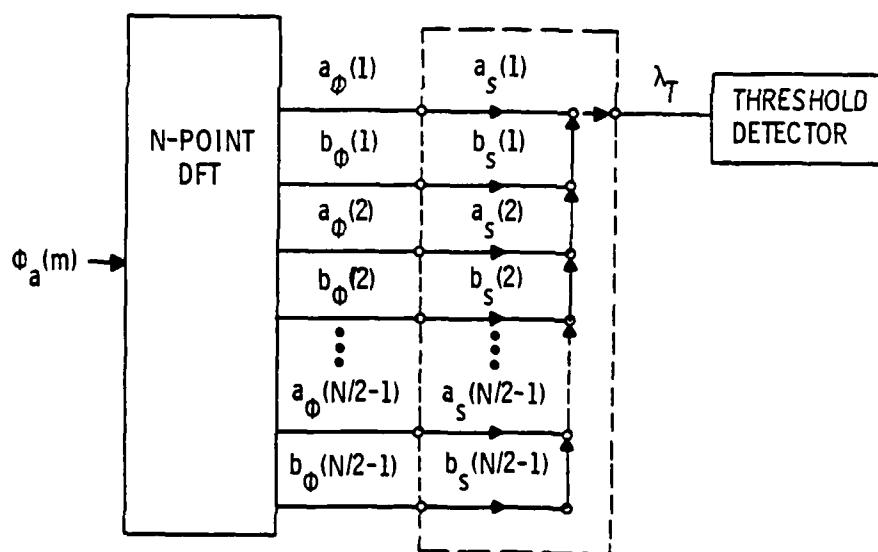
$$\lambda_T = \begin{cases} \frac{1}{N_F} \sum_{k=1}^{\frac{N_F}{2}-1} [a_\phi(k) a_s(k) + b_\phi(k) b_s(k)] , & N \text{ even} \\ \frac{1}{N_F} \sum_{k=1}^{\frac{N_F-1}{2}} [a_\phi(k) a_s(k) + b_\phi(k) b_s(k)] , & N \text{ odd} \end{cases} \quad (2-32)$$

The common multiplier of two has been dropped since it applied to all terms other than $a(0)$ and $a(\frac{N}{2})$. The two versions, complex coefficients and sine-cosine coefficients, of a discrete time matched filter are shown in Figure 2-5.

The output of the matched filter is the input to the threshold detector. The threshold is selected for a given probability of false alarm. If the output exceeds the threshold, hypothesis H_1 is selected and the signal is considered to be present.



(a) COMPLEX COEFFICIENTS



(b) SINE AND COSINE COEFFICIENTS

FIGURE 2-5. Discrete Time Matched Filter Detector.

CHAPTER III

THEORETICAL DEVELOPMENT

In order to establish the receiver performance, it is necessary to know the statistics at the threshold detector. In this chapter, the statistical properties of the random processes are traced through the signal processing system shown in Figure 2-1. The statistical properties of the observable sequences are defined from the signal and noise model. The mean and variance of the average phase estimate is calculated in terms of the signal-to-noise ratio, signal phase, and of the complex correlation coefficient of the noise present in the observable sequences. The statistics of the Fourier coefficient are determined for a non-stationary average phase estimate. From the statistics of the Fourier coefficient, the statistics at the threshold detector are defined and the probability of false alarm and probability of detection determined.

3.1 Input Signal and Noise Characteristics

The statistical properties of the observable complex sequence $r_{p1}(n)$ and $r_{p2}(n)$ given in equations (2-16) can be defined in terms of the signal and noise model described in Chapter II.

The signal is a wide-sense stationary, narrowband, zero-mean, Gaussian stochastic process having a power of σ_s^2 . The mean and variance of the in-phase and quadrature components of the signal are:

$$E\{s_c(t)\} = E\{s_s(t)\} = 0 \quad (3-1)$$

$$E\{s_c^2(t)\} = E\{s_s^2(t)\} = \sigma_s^2 \quad (3-2)$$

$$E\{s_c(t) s_s(t)\} = 0 \quad (3-3)$$

The received noise is correlated, wide-sense stationary, zero-mean, narrowband Gaussian noise with power σ_N^2 . The mean and covariance of the in-phase and quadrature components of the noise are given by equations (2-10) through (2-14).

The observable complex sequences can be defined in terms of the in-phase and quadrature components.

$$\begin{aligned} r_{p1}(n) &= r_{1c}(n) + j r_{1s}(n) \\ r_{p2}(n) &= r_{2c}(n) + j r_{2s}(n) \end{aligned} \quad (3-4)$$

From Equation (2-15):

$$\begin{aligned} r_{1c}(n) &= s_c(n) + N_{1c}(n) \\ r_{1s}(n) &= s_s(n) + N_{1s}(n) \\ r_{2c}(n) &= s_c(n) \cos \phi_s(n) + s_s(n) \sin \phi_s(n) + n_{2c}(n) \\ r_{2s}(n) &= s_c(n) \sin \phi_s(n) + s_s(n) \cos \phi_s(n) + N_{2s}(n) \end{aligned} \quad (3-5)$$

The in-phase and quadrature components of the observable sequences form a vector,

$$\underline{r} = [r_{1c}(n), r_{1s}(n), r_{2c}(n), r_{2s}(n)]' \quad (3-6)$$

with a four-dimensional Gaussian probability density function

$p(r_{1c}, r_{1s}, r_{2c}, r_{2s})$. The covariance matrix of the four-dimensional probability density function can be shown to be:

$$R_r = \sigma_N^2 \begin{bmatrix} 1+h & 0 & \rho_N+h \cos \phi_s & -\lambda_N-h \sin \phi_s \\ 0 & 1+h & \lambda_N+h \sin \phi_s & \rho_N+h \cos \phi_s \\ \rho_N+h \cos \phi_s & \lambda_N+h \sin \phi_s & 1+h & 0 \\ -\lambda_N-h \sin \phi_s & \rho_N+h \cos \phi_s & 0 & 1+h \end{bmatrix} \quad (3-7)$$

$$\text{where } h = \frac{\sigma_s^2}{\sigma_N^2}, \text{ signal-to-noise ratio.} \quad (3-8)$$

The covariance matrix is positive definite. The four-dimensional Gaussian probability density function is:

$$p(\underline{r}) = \frac{1}{(2\pi)^2 |R|^{1/2}} \exp \left(-\frac{1}{2} \underline{r}' R_r^{-1} \underline{r} \right) \quad (3-9)$$

where

$|R_r|$ -- determinant of matrix R_r

R_r^{-1} -- inverse of matrix R_r .

The correlation coefficient of the sequence is

$$K_o e^{j\phi_o} \triangleq \frac{E\{r_1(n)r_2^*(n)\}}{\left[E\{r_1(n)r_1^*(n)\} E\{r_2(n)r_2^*(n)\} \right]^{1/2}} \quad (3-10)$$

Substituting the appropriate terms from the covariance matrix, the correlation coefficient becomes

$$K_o e^{j\phi_o} = \frac{(h \cos \phi_s + \rho_N) + j (h \sin \phi_s + \lambda_N)}{1 + h} \quad (3-11)$$

The magnitude and phase of the correlation coefficient are:

$$K_o^2 = \frac{h^2 + \rho_N^2 + \lambda_N^2 + 2h \cos \phi_s + 2 \lambda_N h \sin \phi_s}{(1 + h)^2} \quad (3-12)$$

$$\phi_o = \tan^{-1} \left(\frac{h \sin \phi_s + \lambda_N}{h \cos \phi_s + \rho_N} \right) \quad (3-13)$$

3.2 Statistical Properties of the Average Phase Estimate

The processes for obtaining the average phase estimates have been described in Chapter II. The average phase statistics will be shown to be a function of the complex correlation coefficient between the two observable sequences $r_{p1}(n)$ and $r_{p2}(n)$.

The phase difference between $r_{p1}(n)$ and $r_{p2}(n)$ has a probability density function given by [15]

$$p(\phi) = \frac{1 - K_o^2}{2\pi} \left\{ \frac{1}{1 - \beta^2} + \frac{\beta}{(1 - \beta^2)^{3/2}} \left(\frac{\pi}{2} + \sin^{-1} \beta \right) \right\} \quad (3-14)$$

where

$$\beta = K_o \cos (\phi - \phi_o), \quad -\frac{\pi}{2} \leq \sin^{-1} \beta \leq \frac{\pi}{2} \quad (3-15)$$

The mean and variance of the single point phase estimate are [16]

$$\bar{\phi} = \frac{\cos^{-1}(K_o \cos \phi_o)}{\sqrt{1 - K_o^2 \cos^2 \phi_o}} K_o \sin \phi_o \quad (3-16)$$

$$\sigma_{\phi}^2 = \frac{\pi^2}{12} - E(K_o) + \cos^{-1}(K_o \cos \phi_o)^2 \frac{(1-K_o^2)}{(1-K_o^2 \cos^2 \phi_o)} \quad (3-17)$$

where

$$E(K_o) = 2 \sum_{n=1}^{\infty} \frac{K_o^{2n}}{(2n)^2} \quad (3-18)$$

The mean and standard deviation of the single phase estimate are plotted as a function of K_o and ϕ_o in Figure 3-1.

3.2.1 Angle Average Phase Estimate

The angle average phase estimate was defined by Equation (2-25). If $\bar{\phi}(n)$ and $\sigma_{\phi}^2(n)$ are constant over the averaging interval, the mean and variance of the angle average phase estimate are [17]

$$\bar{\phi}_{aa} = \bar{\phi}(n) \quad (3-19)$$

$$\sigma_{aa}^2 = \frac{\sigma_{\phi}^2(n)}{N_a} \quad (3-20)$$

These values are also in Figure 3-1. The mean of the angle average phase estimate is independent of the number of points averaged. Thus Figure 3.1(a) also represents the mean of angle average phase estimate plotted as a function of K_o and ϕ_o . Figure 3.1(b) can be considered as a normalized plot of the standard deviation of the angle average phase estimate by labelling the abscissa $N_a \sigma_{aa} / \pi$.

It is assumed that the number of points averaged is large enough so that the central limit theorem may be invoked. This means that the angle average phase estimate can be assumed to have a Gaussian distribution.

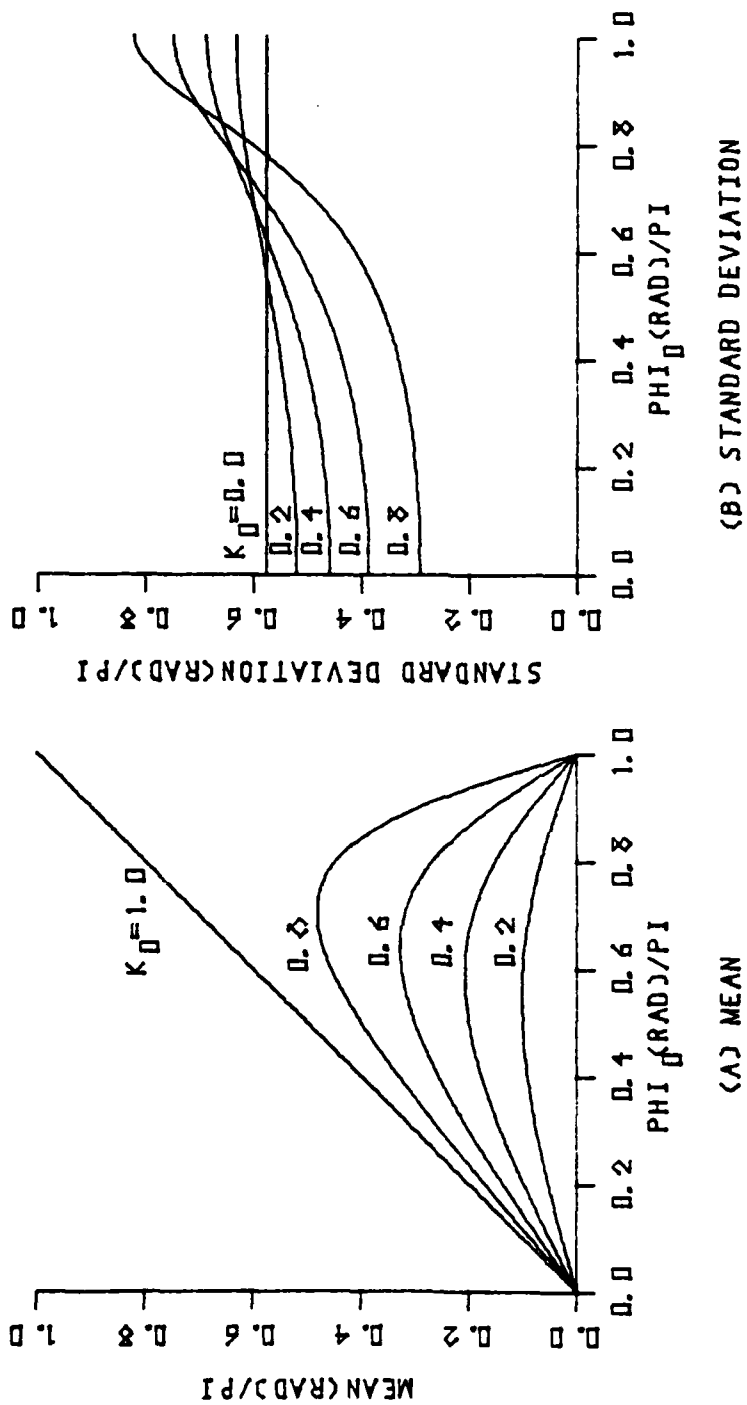


FIGURE 3-1. Mean and Standard Deviation of Single Phase Estimate.

3.2.2 Vector Average Phase Estimate

The vector average phase estimate was described in Chapter II and defined by equation (2-26). Since an expression for the probability density function of the vector average phase estimate is not known, it is necessary to derive such an expression. The mean, variance and correlation coefficient are derived for the real and imaginary components of the complex signal obtained when multiplying complex sequence $r_{p1}(n)$ by the complex conjugate of the complex sequence $r_{p2}(n)$. The real component is considered to be the X vector and the imaginary component is the Y vector. The X and Y vector components are then averaged. It is assumed that the number of points averaged is sufficient to invoke the central limit theorem and consider the average X and average Y vectors to be Gaussian distributed. These variables are shown in Figure 2-4.

An expression is then derived for the probability density function of the vector average phase assuming the average X and average Y vectors are correlated Gaussian parameters with unequal means and variances. Since the expression for the probability density function is not easily integrable, curves of the mean and standard deviation of the vector average phases are generated using numerical techniques.

Expressions for the mean, variance and covariance of the real and imaginary components of the product of a complex variable and the complex conjugate of another complex variable are derived in Appendix A. These expressions are given in terms of the components of the covariance matrix. Substituting the covariance matrix terms from equation (3-7), the equations for the moments of the X and Y vectors become

$$\bar{X} = 2 \sigma_N^2 K_o (1+h) \cos \phi_o \quad (3-21)$$

$$\bar{Y} = 2 \sigma_N^2 K_o (1+h) \sin \phi_o \quad (3-22)$$

$$\sigma_x^2 = 2 \sigma_N^4 (1+h)^2 (1 + K_o^2 \cos 2\phi_o) \quad (3-23)$$

$$\sigma_y^2 = 2 \sigma_N^4 (1+h)^2 (1 - K_o^2 \cos 2\phi_o) \quad (3-24)$$

$$\mu_{xy} = 2 \sigma_N^4 (1+h)^2 K_o^2 \sin 2\phi_o \quad (3-25)$$

The average X and average Y vectors are calculated from

$$X_a = \frac{1}{N_a} \sum_{n=0}^{N_a-1} X(n) \quad (3-26)$$

$$Y_a = \frac{1}{N_a} \sum_{n=0}^{N_a-1} Y(n) \quad (3-27)$$

The moments of X_a and Y_a are

$$\bar{X}_a = \bar{X} \quad (3-28)$$

$$\bar{Y}_a = \bar{Y} \quad (3-29)$$

$$\sigma_{xa}^2 = \frac{\sigma_x^2}{N_a} \quad (3-30)$$

$$\sigma_{ya}^2 = \frac{\sigma_y^2}{N_a} \quad (3-31)$$

$$\mu_a = \frac{\mu_{xy}}{N_a} \quad (3-32)$$

Knowing the moments of the real and imaginary vector components, the vector average phase probability density function can now be derived. Assume the X_a and Y_a vectors are jointly Gaussian distributed, the joint probability density function is given by:

$$p_{xy}(x,y) = \frac{1}{2\pi\sigma_{xa}\sigma_{ya}(1-\rho_{xy}^2)^{1/2}} \exp \left\{ -\frac{1}{2(1-\rho_{xy}^2)} \left[\frac{(X_a - \bar{X}_a)^2}{\sigma_{xa}^2} - 2\rho_{xy} \frac{(X_a - \bar{X}_a)(Y_a - \bar{Y}_a)}{\sigma_{xa}\sigma_{ya}} + \frac{(Y_a - \bar{Y}_a)^2}{\sigma_{ya}^2} \right] \right\} \quad (3-33)$$

The X_a and Y_a vectors are related to the phase angle, ϕ_a and amplitude, r_a by:

$$r = (X_a^2 + Y_a^2)^{1/2} \quad (3-34)$$

$$\phi_{va} = \tan^{-1} \frac{Y_a}{X_a} \quad (3-35)$$

The probability density function of the phase angle, ϕ_{va} , can be determined by finding the joint probability density function of r and ϕ_{va} and then integrating with respect to r . The joint probability density function of r_a and ϕ_{va} can be found from $p_{xy}(x,y)$

$$p(r, \phi_{va}) = \frac{1}{|J|} p_{xy}(r \cos \phi_{va}, r \sin \phi_{va}) \quad (3-36)$$

where

$$J = \begin{vmatrix} \frac{\partial r}{\partial X_a} & \frac{\partial r}{\partial Y_a} \\ \frac{\partial \phi_{va}}{\partial X_a} & \frac{\partial \phi_{va}}{\partial Y_a} \end{vmatrix} \quad (3-37)$$

Substituting Equation (3-34) and (3-35) in (3-37), the Jacobian becomes:

$$J = \frac{1}{\sqrt{X_a^2 + Y_a^2}} = \frac{1}{r} \quad (3-38)$$

The joint probability density function of r and ϕ_{va} then becomes:

$$p(r, \phi_{va}) = \frac{r}{2\pi\sigma_{xa}\sigma_{ya}(1-\rho_{xy}^2)^{1/2}} \exp \left[-\alpha(r, \phi_{va}) \right] \quad (3-39)$$

where

$$\alpha(r, \phi_{va}) = \frac{1}{2} \left[\frac{(r \cos \phi_{va} - \bar{X}_a)^2}{\sigma_{xa}^2} - 2\rho_{xy} \frac{(r \cos \phi_{va} - \bar{X}_a)(r \sin \phi_{va} - \bar{Y}_a)}{\sigma_{xa}\sigma_{ya}} + \frac{(r \sin \phi_{va} - \bar{Y}_a)^2}{\sigma_{ya}^2} \right] \quad (3-40)$$

The probability density function $p(\phi_{va})$ can be found from

$$p(\phi_{va}) = \frac{1}{2\pi\sigma_{xa}\sigma_{ya}(1-\rho_{xy}^2)^{1/2}} \int_{-\infty}^{\infty} r \exp \left[-\alpha(r, \phi_{va}) \right] dr \quad (3-41)$$

Performing the indicated integration and substituting the moments of X_a and Y_a , the vector average phase probability density function becomes

$$\begin{aligned}
p(\phi_{va}) = & \frac{(1-K_o^4)^{1/2}}{2\pi[1-K_o^2 \cos(\phi_{va}-\phi_o)]} \exp\left(-\frac{N_a K_o^2}{1+K_o^2}\right) \\
& + \frac{\sqrt{N_a} K_o (1-K_o^2) \cos(\phi_{va}-\phi_o)}{2\sqrt{\pi} [1-K_o^2 \cos(\phi_{va}-\phi_o)]^{3/2}} \exp\left[-\frac{N_a K_o^2 \sin^2(\phi_{va}-\phi_o)}{1-K_o^2 \cos 2(\phi_{va}-\phi_o)}\right] \\
& \times \left\{ 1 + \operatorname{erf} \left[\frac{\sqrt{N_a} K_o (1-K_o^2)^{1/2} \cos(\phi_{va}-\phi_o)}{(1+K_o^2)^{1/2} [1-K_o^2 \cos 2(\phi_{va}-\phi_o)]^{1/2}} \right] \right\} \quad (3-42)
\end{aligned}$$

where

N_a = number of points averaged

K_o = magnitude of correlation coefficient of the receiver observable sequences $r_{p1}(n)$ and $r_{p2}(n)$ after complex sampling

ϕ_o = phase of correlation coefficient

and

$$\operatorname{erf}(x) = \frac{2}{\sqrt{\pi}} \int_0^x \exp(-Z^2) dZ$$

Probability density functions for the vector average phase are shown in Figure 3-2(a), for various values of K_o when the number of points averaged is held constant, and in Figure 3-2(b), for various values of N_a when K_o is constant. In both figures $p(\phi_{va})$ is plotted as a function of $(\phi_{va}-\phi_o)$ where ϕ_o is the phase angle of the correlation coefficient defined by Equation (3-20). Since the expression for the probability density function is not readily integrable, computer programs were developed to give curves of the mean and variance of the vector average phase estimate as a function of ϕ_o for a given K_o and N_a . Curves of the mean and standard deviation of the vector average phase are shown in Figures (3-3) to (3-6).

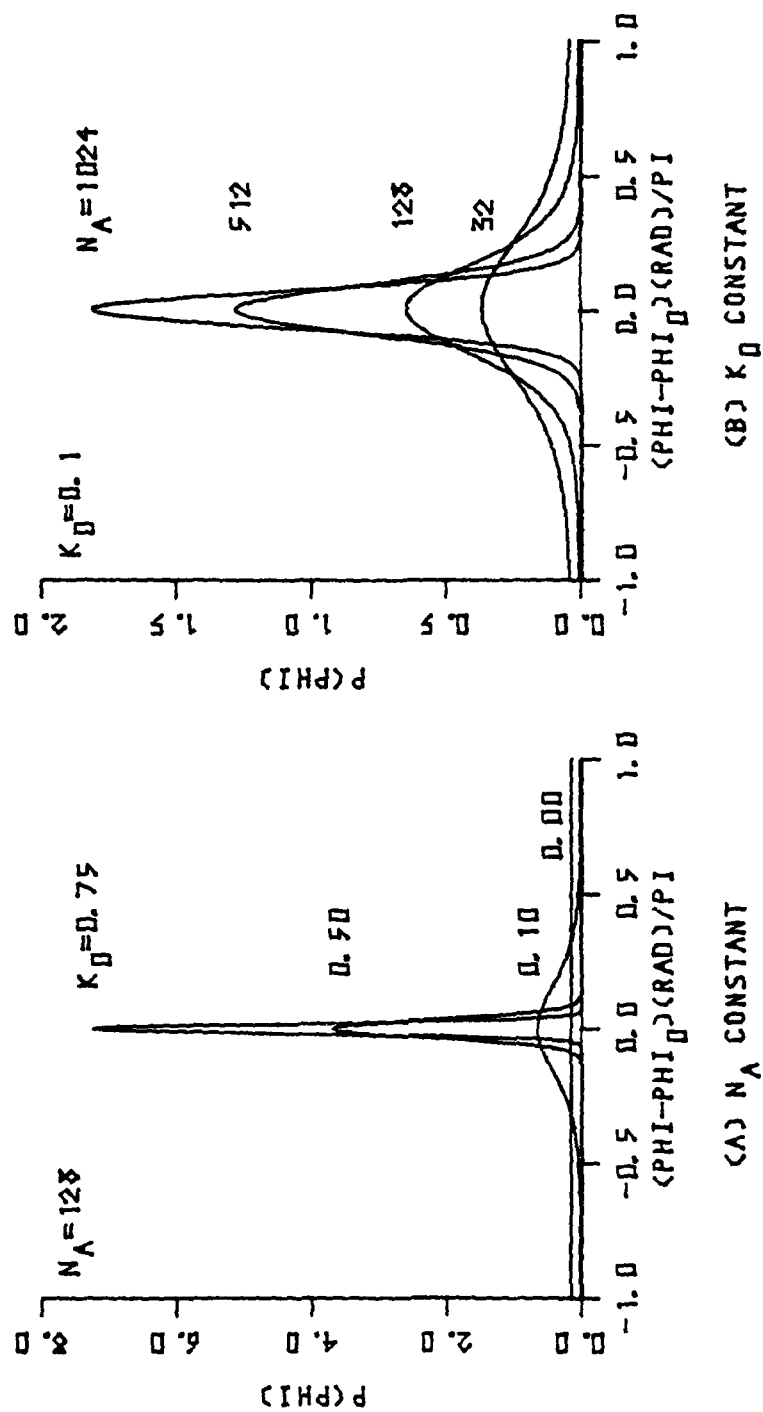


FIGURE 3-2. Probability Density Function of Vector Average Phase Estimate.

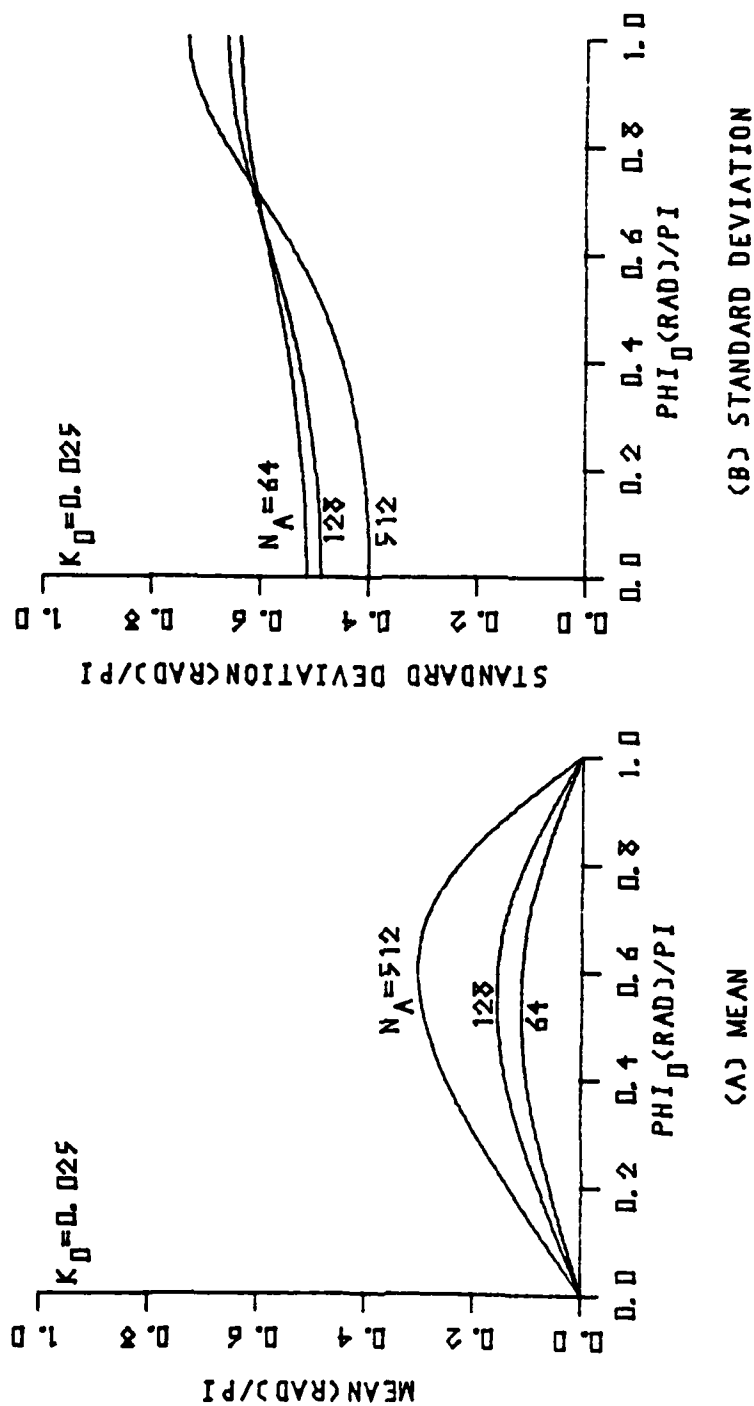


FIGURE 3-3. Mean and Standard Deviation of Vector Average Phase Estimate, $K_0 = 0.025$.

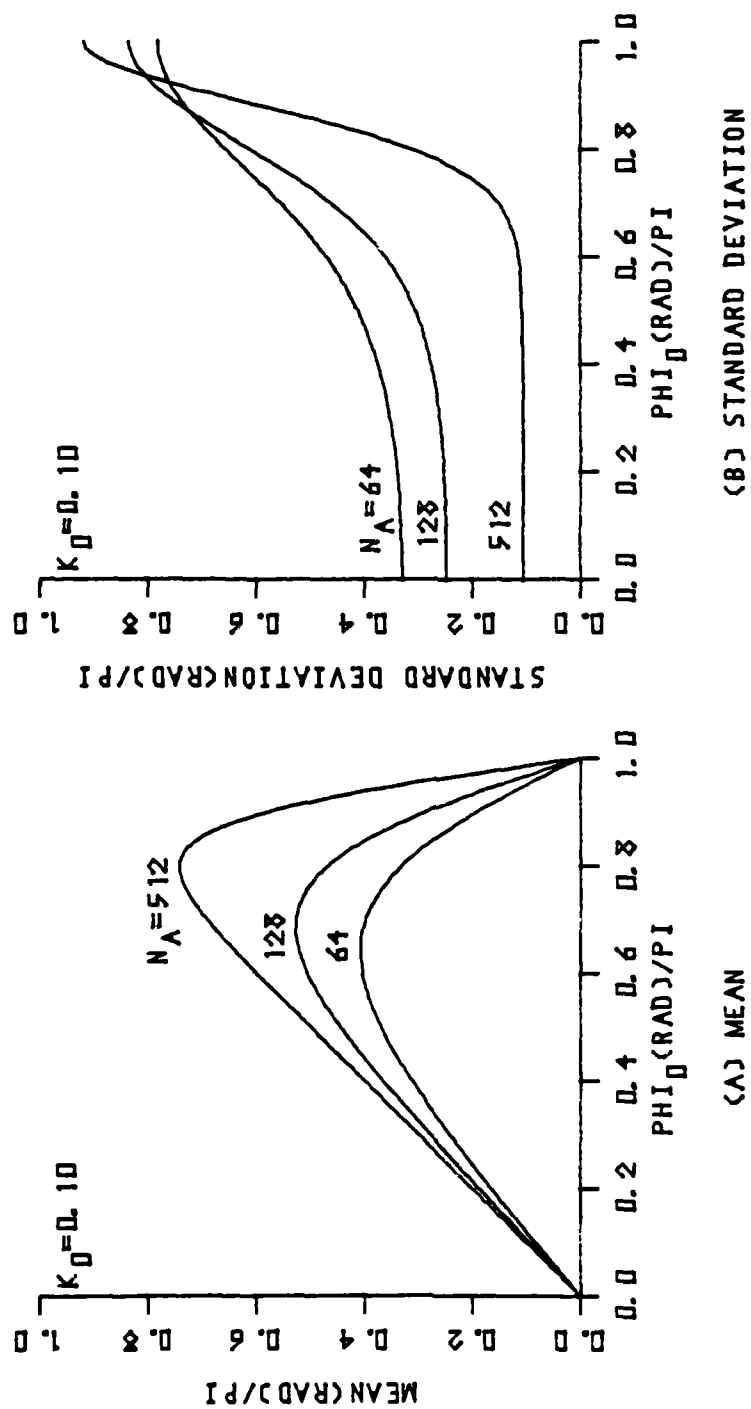


FIGURE 3-4. Mean and Standard Deviation of Vector Average Phase Estimate, $K_0 = 0.10$.

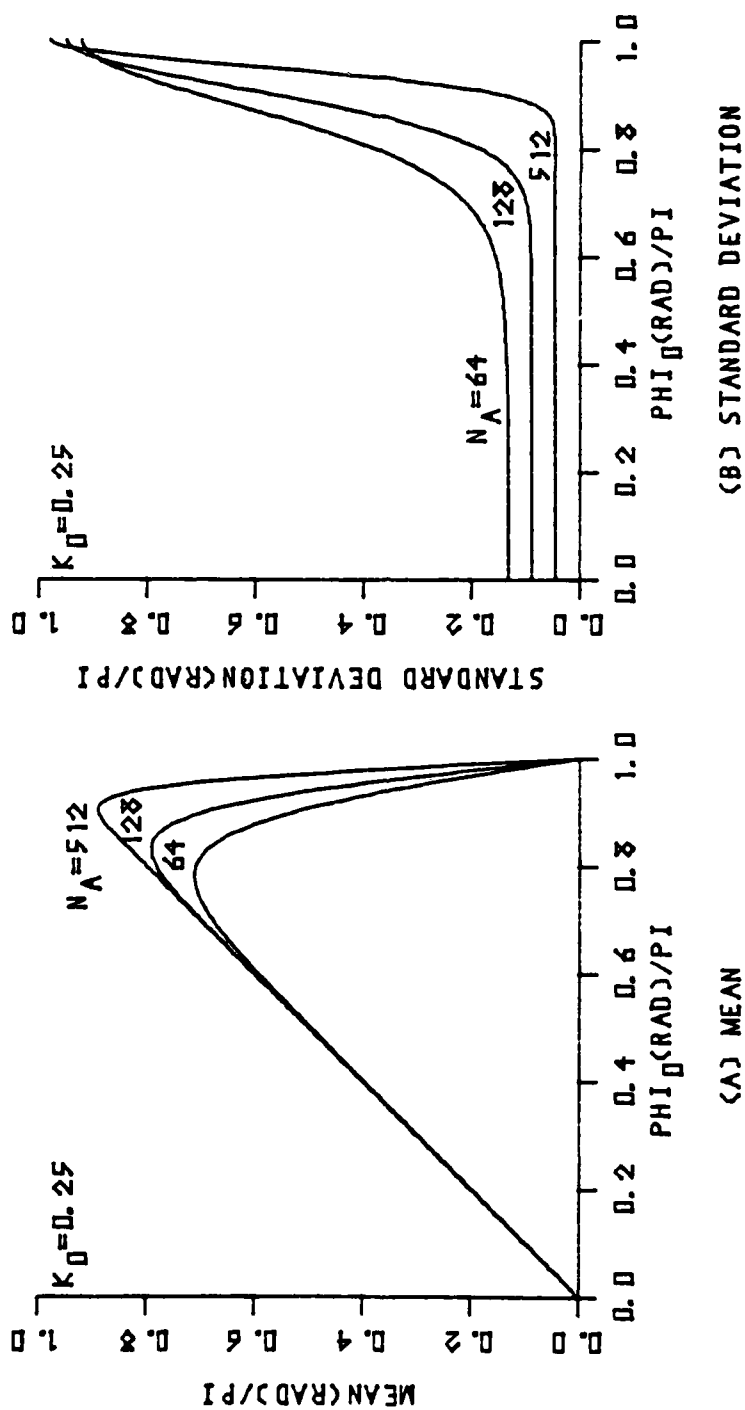


FIGURE 3-5. Mean and Standard Deviation of Vector Average Phase Estimate, $K_0 = 0.25$.

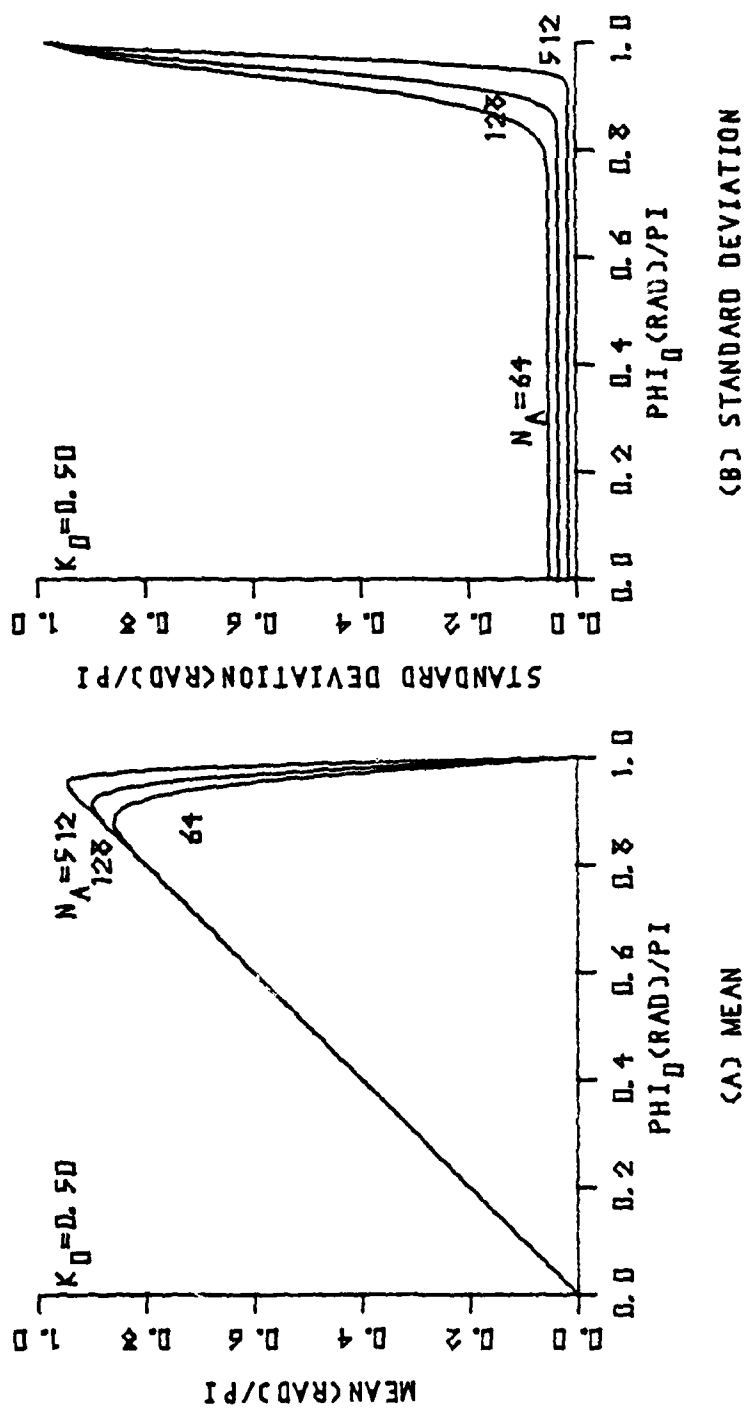


FIGURE 3-6. Mean and Standard Deviation of Vector Average Phase Estimate, $K_0 = 0.50$.

The curves presented are for $K_0 = 0.025, 0.10, 0.25$ and 0.50 and $N = 64, 128, \text{ and } 512$. Values of the mean and standard deviation for other values of K_0 and N can be obtained by interpolating from the curves presented.

3.3 Statistics of the Fourier Coefficient for Non-Stationary Periodic Input

The matched filter detector was described in Chapter II and shown in Figure 2-5. The first function performed by the matched filter detector is a Discrete Fourier Transform of the average phase estimate $\phi_a(m)$. The mean and standard deviation of the average phase estimate are known. The standard deviation is a function of the signal phase which changes with time. Therefore, the input to the DFT must be considered to be a non-stationary process.

The real, discrete time sequence $\phi_a(m)$ is a non-stationary random process with mean, $\overline{\phi_a(m)}$, and variance, $\sigma_{\phi_a}^2(m)$. The mean and variance are known for values of m between zero and (N_F-1) . Over this period, the mean and variance of $\phi_a(m)$ can be expanded by a Discrete Fourier Transform,

$$\overline{\phi_a(m)} = \frac{1}{N_F} \sum_{k=0}^{N_F-1} C_m(k) e^{j \frac{2\pi km}{N_F}}, \quad 0 \leq m \leq N_F-1 \quad (3-43)$$

or

$$\begin{aligned} \overline{\phi_a(m)} &= \frac{1}{N_F} \sum_{k=0}^{N_F-1} a_m(k) \cos \frac{2\pi km}{N_F} + \\ &\quad \frac{1}{N_F} \sum_{k=0}^{N_F-1} b_m(k) \sin \frac{2\pi km}{N_F}, \quad 0 \leq m \leq N_F-1 \end{aligned} \quad (3-44)$$

where

$$\begin{aligned}
 c_m(k) &= \sum_{m=0}^{N_F-1} \overline{\phi_a(m)} e^{-j \frac{2\pi km}{N_F}}, \quad 0 \leq k \leq N_F-1 \\
 a_m(k) &= \sum_{m=0}^{N_F-1} \overline{\phi_a(m)} \cos \frac{2\pi km}{N_F}, \quad 0 \leq k \leq N_F-1 \\
 b_m(k) &= \sum_{m=0}^{N_F-1} \overline{\phi_a(m)} \sin \frac{2\pi km}{N_F}, \quad 0 \leq k \leq N_F-1
 \end{aligned} \tag{3-45}$$

and

$$\sigma_{\phi_a}^2(m) = \frac{1}{N} \sum_{k=0}^{N_F-1} c_v(k) e^{j \frac{2\pi km}{N_F}}, \quad 0 \leq m \leq N_F-1 \tag{3-46}$$

or

$$\begin{aligned}
 \sigma_{\phi_a}^2(m) &= \frac{1}{N_F} \sum_{K=0}^{N_F-1} a_v(k) \cos \frac{2\pi km}{N_F} \\
 &\quad + \frac{1}{N_F} \sum_{k=0}^{N_F-1} b_v(k) \sin \frac{2\pi km}{N_F}, \quad 0 \leq m \leq N_F-1
 \end{aligned} \tag{3-47}$$

where

$$\begin{aligned}
 c_v(k) &= \sum_{m=0}^{N_F-1} \sigma_{\phi a}^2(m) e^{-j \frac{2\pi km}{N}}, \quad 0 \leq k \leq N_F-1 \\
 a_v(k) &= \sum_{m=0}^{N_F-1} \sigma_{\phi a}^2(m) \cos \frac{2\pi km}{N}, \quad 0 \leq k \leq N_F-1 \\
 b_v(k) &= \sum_{m=0}^{N_F-1} \sigma_{\phi a}^2(m) \sin \frac{2\pi km}{N}, \quad 0 \leq k \leq N_F-1
 \end{aligned} \tag{3-48}$$

Sequential samples of the random sequence are assumed to be independent.

The discrete time sequence, $\phi_a(m)$, can also be expanded by a Discrete Fourier Transform over the period N_F . It is necessary to know the moments of the resulting Fourier coefficient; $c_\phi(k)$, $a_\phi(k)$, and $b_\phi(k)$; to establish the statistical performance of the matched filter detector. These Fourier coefficients are:

$$\begin{aligned}
 c_\phi(k) &= \sum_{m=0}^{N_F-1} \phi_a(m) e^{-j \frac{2\pi km}{N_F}}, \quad 0 \leq k \leq N_F-1 \\
 a_\phi(k) &= \sum_{m=0}^{N_F-1} \phi_a(m) \cos \frac{2\pi km}{N_F}, \quad 0 \leq k \leq N_F-1 \\
 b_\phi(k) &= \sum_{m=0}^{N_F-1} \phi_a(m) \sin \frac{2\pi km}{N_F}, \quad 0 \leq k \leq N_F-1
 \end{aligned} \tag{3-49}$$

3.3.1 Mean Value of the Fourier Coefficient

The mean value of a linear summation of random variables is equal to the linear summation of the mean values of the random variables. Therefore, the mean values of the Fourier Coefficients in equation (3-49) are equal to the right-hand side of equation (3-45). Thus

$$\left. \begin{aligned} \overline{C_{\phi}(k)} &= C_m(k) \\ \overline{a_{\phi}(k)} &= a_m(k) \\ \overline{b_{\phi}(k)} &= b_m(k) \end{aligned} \right\} \quad (3-50)$$

The mean of the Fourier coefficients for the DFT representation of $\phi_a(n)$ is equal to the respective Fourier coefficients of the DFT expansion of the mean $\overline{\phi_a(m)}$ of the random sequence.

3.3.2 Variance of the Fourier Coefficients

The variance of a linear summation of uncorrelated random variables is equal to the summation of the squares of the linear coefficients times the variance of each random variable. Therefore, variance of the Fourier coefficients is given by:

$$\begin{aligned}
 \sigma_c^2(k) &= \sum_{m=0}^{N_F-1} \sigma_{\phi a}^2(m) \\
 \sigma_a^2(k) &= \sum_{m=0}^{N_F-1} \sigma_{\phi a}^2(m) \left(\cos \frac{2\pi km}{N_F} \right)^2 \\
 \sigma_b^2(k) &= \sum_{m=0}^{N_F-1} \sigma_{\phi a}^2(m) \left(\sin \frac{2\pi km}{N_F} \right)^2
 \end{aligned} \tag{3-51}$$

The right-hand side of the equation for the exponential coefficient is the DC term of the discrete Fourier Transform expansion of the variance of the random sequence $\phi_a(m)$ [see Equation (3-48) with k set equal to zero]. Therefore,

$$\sigma_c^2(k) = C_v(0) \tag{3-52}$$

Replacing the squared terms in Equations (3-51) with their respective trigonometric identity, the variance of the sine and cosine coefficients become:

$$\begin{aligned}
 \sigma_a^2(k) &= \frac{1}{2} \sum_{m=0}^{N_F-1} \sigma_x^2(m) + \frac{1}{2} \sum_{m=0}^{N_F-1} \sigma_x^2(m) \cos \frac{4\pi km}{N_F} \\
 \sigma_b^2(k) &= \frac{1}{2} \sum_{m=0}^{N_F-1} \sigma_x^2(m) - \frac{1}{2} \sum_{m=0}^{N_F-1} \sigma_x^2(m) \cos \frac{4\pi km}{N_F}
 \end{aligned} \tag{3-53}$$

The first term in the above equation is one half the DC term in the DFT expansion of the variance of the random sequence $\phi_a(m)$. Comparing the second term with Equation (3-48), it is easily shown that

$$\sum_{m=0}^{N_F-1} \sigma_x^2(m) \cos \frac{4\pi km}{N_F} = \begin{cases} a_v(0) = C_v(0) , & k=0 \\ a_v(2k) , & 1 \leq k < \frac{N_F}{2} \\ a_v(0) = C_v(0) , & k = \frac{N_F}{2} \\ a_v(2k-N_F) , & \frac{N_F}{2} < k \leq N_F-1 \end{cases} \quad (3-54)$$

Therefore, the expression for the variance becomes:

$$\sigma_a^2(k) = \begin{cases} c_v(0) , & k=0, \frac{N_F}{2} \\ \frac{1}{2} [c_v(0) + a_v(2k)] , & 1 \leq k < \frac{N_F}{2} \\ \frac{1}{2} [c_v(0) + a_v(2k-N_F)] , & \frac{N_F}{2} < k \leq N_F-1 \end{cases} \quad (3-55)$$

$$\sigma_b^2(k) = \begin{cases} c_v(0) , & k=0, \frac{N_F}{2} \\ \frac{1}{2} [c_v(0) - a_v(2k)] , & 1 \leq k < \frac{N_F}{2} \\ \frac{1}{2} [c_v(0) - a_v(2k-N_F)] , & \frac{N_F}{2} < k \leq N_F-1 \end{cases} \quad (3-56)$$

3.3.3 Correlation of the Sine and Cosine Coefficients

The covariance between the sine and cosine coefficients is given by

$$\begin{aligned} \mu_{ab}(k) &= \sum_{n=0}^{N_F-1} \sum_{m=0}^{N_F-1} E \{ \phi_a(n) \phi_a(m) \} \cos \frac{2\pi kn}{N_F} \sin \frac{2\pi km}{N_F} \\ &= \overline{a(k)} \overline{b(k)} \end{aligned}$$

Sequential samples of the random sequence are independent; therefore the covariance is:

$$\mu_{ab}(k) = \frac{1}{2} \sum_{m=0}^{N_F-1} \sigma_x^2(m) \sin \frac{4\pi km}{N_F} \quad (3-57)$$

Comparing the right-hand term of Equation (3-56) with Equation (3-48), the expression for the covariance becomes

$$\mu_{ab}(k) = \begin{cases} 0 & , k=0, \frac{N_F}{2} \\ \frac{1}{2} b_v(2k) & , 1 \leq k < \frac{N_F}{2} \\ \frac{1}{2} b_v(2k-n), & \frac{N_F}{2} < k \leq N_F-1 \end{cases} \quad (3-58)$$

3.3.4 Correlation Between Fourier Coefficients of Different Harmonics

The covariance terms between Fourier Coefficients of different harmonics are:

$$\mu_c(k, l) = E \{ c(k) c^*(l) \} - \overline{c(k)} \overline{c(l)}$$

$$\mu_a(k, l) = E \{ a(k) a(l) \} - \overline{a(k)} \overline{a(l)}$$

$$\mu_b(k, l) = E \{ b(k) b(l) \} - \overline{b(k)} \overline{b(l)}$$

$$\mu_{ab}(k, l) = E \{ a(k) b(l) \} - \overline{a(k)} \overline{b(l)}$$

Substituting

$$\mu_c(k, l) = \sum_{m=0}^{N_F-1} \sigma_{\phi a}^2(m) e^{-j \frac{2\pi(k-l)m}{N_F}}$$

$$\mu_a(k, l) = \frac{1}{2} \sum_{m=0}^{N_F-1} \sigma_{\phi a}^2(m) \cos \frac{2\pi(k+l)m}{N_F} + \frac{1}{2} \sum_{m=0}^{N_F-1} \sigma_{\phi a}^2(m) \cos \frac{2\pi(k-l)m}{N_F}$$

$$\mu_b(k, l) = \frac{1}{2} \sum_{m=0}^{N_F-1} \sigma_{\phi a}^2(m) \cos \frac{2\pi(k-l)m}{N_F} - \frac{1}{2} \sum_{m=0}^{N_F-1} \sigma_{\phi a}^2(n) \cos \frac{2\pi(k+l)m}{N_F}$$

$$\mu_{ab}(k, l) = \frac{1}{2} \sum_{m=0}^{N_F-1} \sigma_{\phi a}^2(m) \sin \frac{2\pi(k+l)m}{N_F} + \frac{1}{2} \sum_{m=0}^{N_F-1} \alpha_{\phi a}^2(n) \sin \frac{2\pi(k-l)m}{N_F}$$

Comparing the above equations with Equations (3-48), the covariance expressions become

$$\begin{aligned}
 \mu_c(k, \ell) &= c_v(k-\ell) \\
 \mu_a(k, \ell) &= \frac{1}{2} a_v(k-\ell) + \frac{1}{2} a_v(k+\ell) \\
 \mu_b(k, \ell) &= \frac{1}{2} a_v(k-\ell) - \frac{1}{2} a_v(k+\ell) \\
 \mu_{ab}(k, \ell) &= \frac{1}{2} b_v(k+\ell) - \frac{1}{2} b_v(k-\ell)
 \end{aligned}
 \tag{3-59}$$

3.3.5 Distribution of the Fourier Coefficients

The sine and cosine Fourier coefficients are formed by a linear transformation of random variables. Therefore, the Fourier coefficients are also random variables and they have a Gaussian limiting distribution. For the cases under consideration it will be assumed that N_F is large enough that the central limit theorem applies and the distribution of the sine and cosine Fourier Coefficients can be considered to be Gaussian with mean and variance as previously derived.

The moments of the Fourier coefficients for the real discrete, random sequence $\phi_a(m)$ are summarized in Table 3-1. If the Fourier Coefficients of the DFT expansion of the variance of sequence $\phi_a(m)$ has a DC term which is large with respect to any of the higher order coefficients, the input sequence can be considered to be stationary. For a stationary sequence, the moments given in Table 3-1 can be simplified as

TABLE 3-1

MOMENTS FOR FOURIER COEFFICIENTS OF NON-STATIONARY SEQUENCE

	$k = 0$	$1 \leq k \leq (\frac{N}{2} - 1)$	$k = \frac{N}{2}$	$(\frac{N}{2} + 1) \leq k \leq (N-1)$
$\overline{C(k)}$	$C_m(0)$	$C_m(k)$	$C_m(\frac{N}{2})$	$C_m(k)$
$\sigma_c^2(k)$	$C_v(0)$	$C_v(0)$	$C_v(0)$	$C_v(0)$
$\mu_c(k, l)$	$C_v(-l)$	$C_v(k-l)$	$C_v(\frac{N}{2} - l)$	$C_v(k-l)$
$\overline{a(k)}$	$a_m(0)$	$a_m(k)$	$a_m(\frac{N}{2})$	$a_m(k)$
$\sigma_a^2(k)$	$C_v(0)$	$\frac{C_v(0) + a_v(2k)}{2}$	$C_v(0)$	$\frac{C_v(0) + a_v(2k-N)}{2}$
$\overline{b(k)}$	0	$b_m(k)$	0	$b_m(k)$
$\sigma_b^2(k)$	0	$\frac{C_v(0) - a_v(2k)}{2}$	0	$\frac{C_v(0) - a_v(2k-N)}{2}$
$\rho_{ak}(k)$	0	$\frac{b_v(2k)}{[C_v^2(0) - a_v^2(2k)]^{1/2}}$	0	$\frac{b_v(2k-N)}{[C_v^2(0) - a_v^2(2k-N)]^{1/2}}$
$\mu_a(k, l)$	$a_v(l)$	$\frac{a_v(k-l) + a_v(k+l)}{2}$	$a_v(\frac{N}{2} - l)$	$\frac{a_v(k-l) + a_v(k+l)}{2}$
$\mu_b(k, l)$	0	$\frac{a_v(k-l) - a_v(k+l)}{2}$	0	$\frac{a_v(k-l) - a_v(k+l)}{2}$
$\mu_{a,b}(k, l)$	$b_v(l)$	$\frac{b_v(k+l) - b_v(k-l)}{2}$	$b_v(\frac{N}{2} - l)$	$\frac{b_v(k+l) - b_v(k-l)}{2}$

$$C_m(k) = \sum_{m=0}^{N_F-1} \overline{\phi_a(m)} e^{-j \frac{2\pi km}{N_F}}$$

$$a_m(k) = \sum_{m=0}^{N_F-1} \overline{\phi_a(m)} \cos \frac{2\pi km}{N_F}$$

$$b_m(k) = \sum_{m=0}^{N_F-1} \overline{\phi_a(m)} \sin \frac{2\pi km}{N_F}$$

$$C_v(k) = \sum_{m=0}^{N_F-1} \sigma_{\phi_a}^2(m) e^{-j \frac{2\pi km}{N_F}}$$

$$a_v(k) = \sum_{m=0}^{N_F-1} \sigma_{\phi_a}^2(m) \cos \frac{2\pi km}{N_F}$$

$$b_v(k) = \sum_{m=0}^{N_F-1} \sigma_{\phi_a}^2(m) \sin \frac{2\pi km}{N_F}$$

given in Table 3-2.

3.4 Statistics of Threshold Detector Input

The output of the matched filter is given by the equation (2-31). This parameter is the input to the threshold detector which determines if the desired signal is present. The mean value of the threshold detector input is

$$\bar{\lambda}_T = \sum_{k=1}^K [a_s(k) \overline{a(k)} + b_s(k) \overline{b(k)}] \quad (3-60)$$

where:

$$K = \begin{cases} \frac{N}{2} - 1, & N \text{ even} \\ \frac{N-1}{2}, & N \text{ odd} \end{cases}.$$

The variance can be found from

$$\sigma_{\lambda}^2 = \overline{\lambda_T^2} - \bar{\lambda}_T^2$$

Expanding, the variance of λ_T becomes

$$\begin{aligned} \sigma_{\lambda}^2 = & \sum_{k=1}^K [a_s^2(k) \sigma_a^2(k) + b_s^2(k) \sigma_b^2(k) + 2a_s(k) b_s(k) \mu_{ab}(k)] \\ & + \sum_{k=1}^K \sum_{\substack{\ell=1 \\ \ell \neq k}}^K [a_s(k) a_s(\ell) \mu_a(k, \ell) + b_s(k) b_s(\ell) \mu_b(k, \ell) \\ & + 2 a_s(k) b_s(\ell) \mu_{ab}(k, \ell)] \end{aligned} \quad (3-61)$$

TABLE 3-2

APPROXIMATE VALUE FOR MOMENTS OF FOURIER COEFFICIENTS
ASSUMING STATIONARY INPUT SEQUENCE

	$k = 0$	$1 \leq k \leq (\frac{N}{2} - 1)$	$k = \frac{N}{2}$	$(\frac{N}{2} + 1) \leq k \leq (N - 1)$
$\overline{c(k)}$	$C_m(k)$	$C_m(k)$	$C_m(k)$	$C_m(k)$
$\sigma_c^2(k)$	$C_v(0)$	$C_v(0)$	$C_v(0)$	$C_v(0)$
$\rho_c(k, l)$	0	0	0	0
$\overline{a(k)}$	$a_m(k)$	$a_m(k)$	$a_m(k)$	$a_m(k)$
$\sigma_a^2(k)$	$C_v(0)$	$\frac{C_v(0)}{2}$	$C_v(0)$	$\frac{C_v(0)}{2}$
$\rho_a(k, l)$	0	0	0	0
$\overline{b(k)}$	0	$b_m(k)$	0	$b_m(k)$
$\sigma_b^2(k)$	0	$\frac{C_v(0)}{2}$	0	$\frac{C_v(0)}{2}$
$\rho_b(k, l)$	0	0	0	0
$\rho_{ab}(k, l)$	0	0	0	0

$$C_m(k) = \sum_{m=0}^{N_F-1} \overline{X(m)} e^{-j \frac{2\pi km}{N_F}}$$

$$a_m(k) = \sum_{m=0}^{N_F-1} \overline{X(m)} \cos \frac{2\pi km}{N_F}$$

$$b_m(k) = \sum_{m=0}^{N_F-1} \overline{X(m)} \sin \frac{2\pi km}{N_F}$$

$$C_v(0) = \sum_{m=0}^{N_F-1} \sigma_x^2(m)$$

where the values of the variance and covariance terms can be found in Tables 3-1 or 3-2. Since the Fourier coefficients are assumed to be Gaussian, the input to the threshold detector is also Gaussian.

$$P(\lambda_T) = \frac{1}{\sqrt{2\pi} \sigma_\lambda} \exp \left[-\frac{(\lambda_T - \bar{\lambda}_T)^2}{2\sigma_\lambda^2} \right] \quad (3-62)$$

The probability that λ_T will exceed the threshold is

$$P(\lambda_T > \lambda_{TH}) = \frac{1}{2} \left[1 - \text{erf} \left(\frac{\lambda_{TH} - \bar{\lambda}_T}{\sqrt{2} \sigma_\lambda} \right) \right] \quad (3-63)$$

The likelihood functions can be obtained from the probability density function of λ_T

$$P_0(\lambda_T) = P(\lambda_T \leq \lambda_T \leq \lambda_T + d\lambda_T | H_0) \quad (3-64)$$

$$P_1(\lambda_T) = P(\lambda_T \leq \lambda_T \leq \lambda_T + d\lambda_T | H_1) \quad (3-65)$$

3.5 Receiver Operating Characteristics

The receiver operating characteristics, ROC, curves relate the probability of detection versus the probability of false alarm for a given signal-to-noise ratio. These curves can be determined from the properties of the desired signal, the signal phase, the properties of the correlated noise and the signal-to-noise ratio. The likelihood ratios can be found in the following manner:

1. Determine the input noise correlation coefficients ρ_N and λ_N ; the signal-to-noise ratio h and the phase $\phi_s(t)$, of the desired signal.

2. Calculate the observable signal correlation coefficient magnitude K_0 and phase ϕ_0 using Equations (3-12) and (3-13). Values of K_0 and ϕ_0 should be calculated over the total processing interval (or sequence period).
3. Determine the mean and variance of the average phase over the total processing interval. NOTE: it is assumed the averaging time is short enough that the signal phase can be considered constant during the averaging interval.
4. Calculate the Fourier coefficients for the mean and variance of the average phase.
5. Calculate the statistical moments of the DFT coefficients using Table (3-1) [Table (3-2) if the average phase variance is independent of time].
6. Determine the mean and variance of the threshold detector input using Equations (3-60) and (3-61).
7. The likelihood function is calculated using Equation (3-62).

For the H_0 hypothesis, the mean and variance of the average phase will be constant over the processing period. The input to the matched filter is stationary and the values for the moments of DFT coefficients are:

$$\overline{c(k)} = 0, \quad k \neq 0 \quad (3-66)$$

$$\sigma_a^2(k) = \sigma_b^2(k) = \frac{N_F \sigma_{\phi a}}{2} \quad (3-67)$$

where

$\sigma_{\phi a}^2$ - variance of average phase estimate given H_0

N_F - number of points in DFT.

The mean and variance of the threshold detector input are:

$$\overline{\lambda_{To}} = 0 \quad (3-68)$$

$$\sigma_{\lambda o}^2 = \frac{N_F \sigma_{\phi a}^2}{2} \sum_{k=1}^K [a_s^2(k) + b_s^2(k)] \quad (3-69)$$

and the likelihood ratio is:

$$p_o(\lambda_T) = \frac{1}{\sqrt{2\pi} \sigma_{\lambda o}} \exp \left(- \frac{\lambda_T^2}{2\sigma_{\lambda o}^2} \right) \quad (3-70)$$

The probability of false alarm is:

$$p_{fa} = \frac{1}{2} \left[1 - \operatorname{erf} \left(\frac{\lambda_T}{\sqrt{2} \sigma_{\lambda o}} \right) \right] \quad (3-71)$$

The likelihood ratio for the H_1 hypothesis can be found using the steps given. The probability of detection can then be determined from the $p_1(\lambda_T)$ likelihood function.

CHAPTER IV

DETECTION OF KNOWN SIGNALS

The preceding chapters described a receiver to detect a dual channel differential phase modulated signal and developed the theoretical results necessary to determine the receiver operating characteristic curves. In this chapter we will apply those results to the detection of "known signals." "Known signals" is used to mean signals as described in Chapter II with a known signal phase delay function. One example will be examined. The example is a linear delay which is often encountered in a practical application. Radiation from a source moving with a constant velocity will result in an approximate linear phase delay between the output of two spatially separated sensors. The matched filter configuration is determined, the mean and variance of the average phase estimate calculated in both the time domain and the frequency domain, and the ROC curves developed. The average phase estimate is calculated for both the angle average and vector average cases so that the effect of the averaging method on the receiver operating characteristics can be examined.

Detection of these known signals is evaluated under varying noise correlation conditions. The magnitude, K_N , and phase, ϕ_N , of the noise correlation coefficients considered are:

$$K_N = 0$$

$$K_N = 0.5, \quad \phi_N = 0$$

$$K_N = 0.5, \quad \phi_N = \frac{\pi}{2}$$

$$K_N = 0.7, \quad \phi_N = \frac{\pi}{4}$$

$$K_N = 0.2, \quad \phi_N = \pi$$

Two cases are investigated using the preceding correlated noise conditions. For the first case, the noise correlation is known a priori allowing the detection threshold to be fixed for a desired false alarm rate. In the second case, the noise correlation is unknown a priori and the threshold is set based on an assumed correlation condition. The analytical ROC curves are generated for two threshold settings.

The examples considered have 6400 points in the processing interval and each interval represents one period of the time delay function. The 6400 points are processed by averaging 100 points and performing a 64-point DFT. No attempt is made to investigate an optimum trade-off between the number of points averaged and number of points in the DFT.

4.1 Linear Delay With Known Noise Correlation

The linear (or ramp) phase delay function is:

$$\phi_s(t) = \phi_p \left(-1 + \frac{2t}{T} \right), \quad 0 \leq t \leq T.$$

The phase delay of the sampled signal becomes:

$$\phi_s(n) = \phi_p(-1 + \frac{2n}{N}), \quad 0 \leq n \leq N-1 \quad . \quad (4-1)$$

For the example being investigated ϕ_p was chosen to be $\pi/2$ radians (90°).

The Fourier transform of the linear delay is:

$$a_s(k) = 0 \quad (4-2)$$

$$b_s(k) = -\frac{\phi_p N_F}{\pi k}, \quad 1 \leq k \leq N_F-1 \quad . \quad (4-3)$$

The configuration used in implementing the filter is an approximation of the ideal matched filter in that only the first three harmonics are used as shown in Figure 4-1. The configuration was chosen to simplify implementation and because after the averaging process the higher harmonics fall off faster than the inverse of k .

The likelihood functions are again found using the procedure from Chapter III. The steps will not be presented in detail. Any approximations will be discussed and the results presented.

Figures 4-2 through 4-4 show the correlation coefficient between the observable signals, the angle average mean and variance and the vector average mean and variance, respectively. These variables are all shown for a signal-to-noise ratio of -12 dB.

The mean and variance of the input to the threshold detector are based on the first three harmonics. The mean of λ_T is:

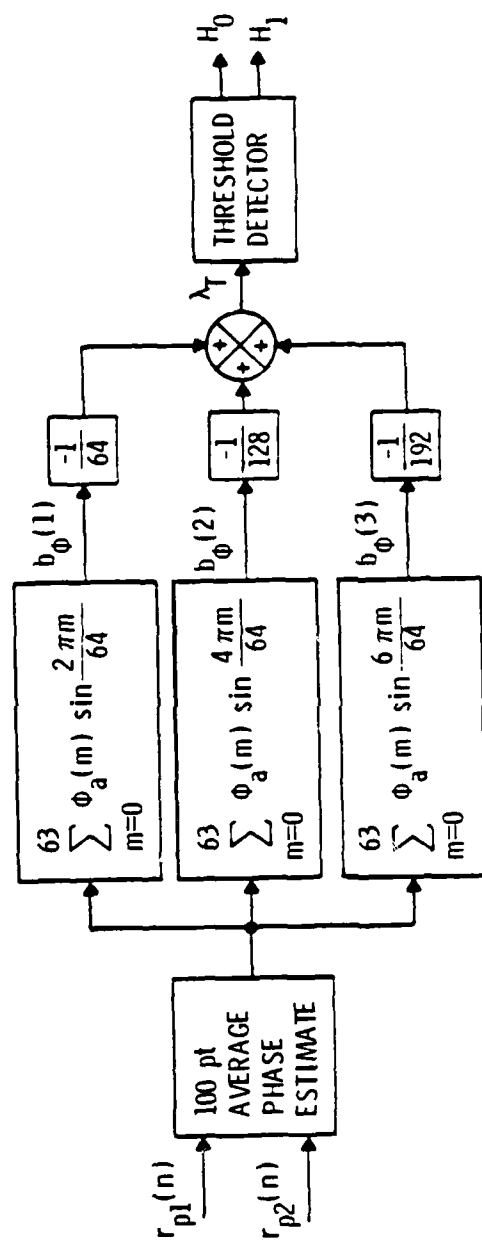


FIGURE 4-1. Approximate Matched Filter Configuration for Linear Delay.

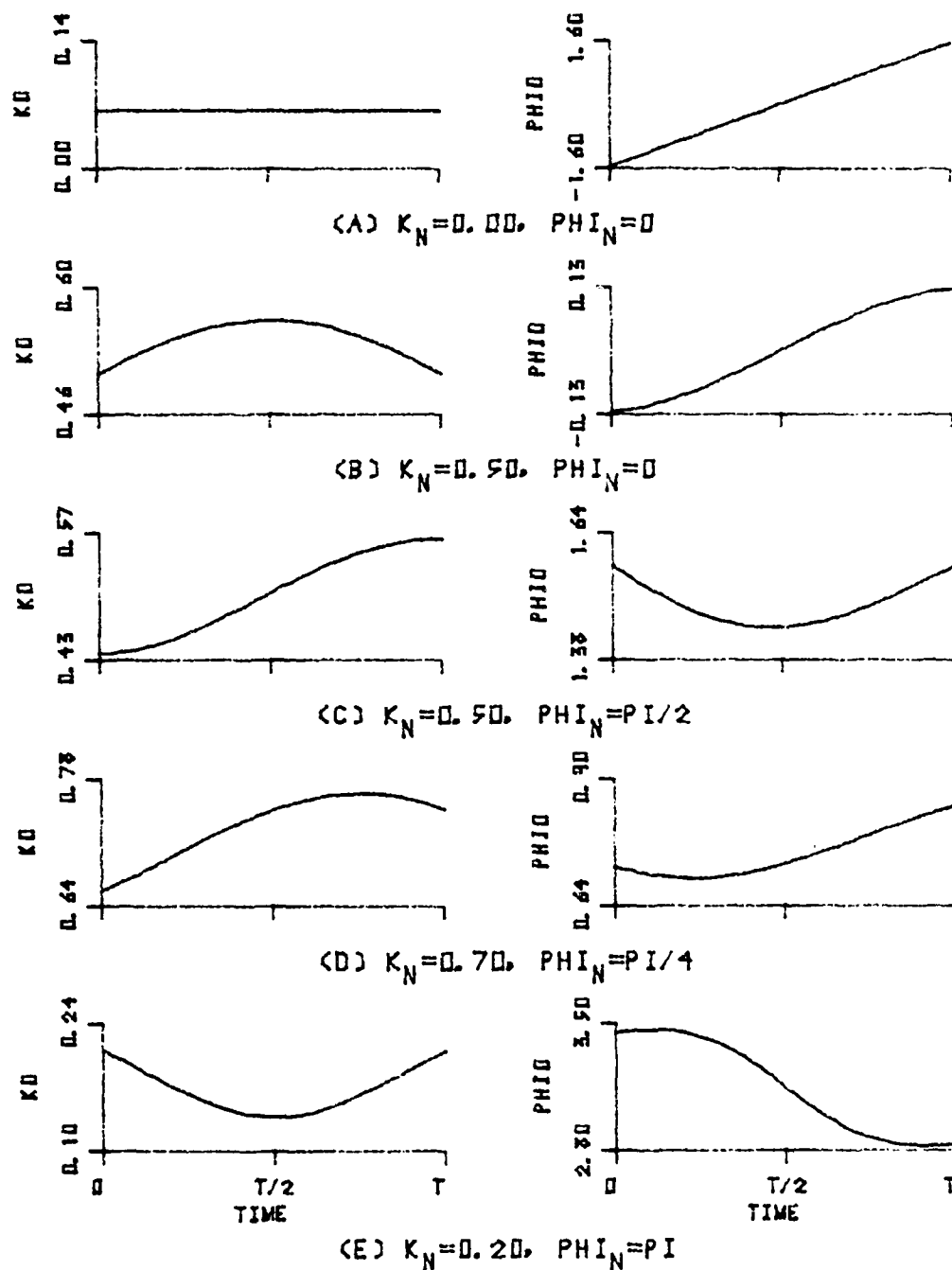


FIGURE 4-2. Variation in K_0 and ϕ_0 for Linear Delay and $\text{SNR} = -12$ dB.

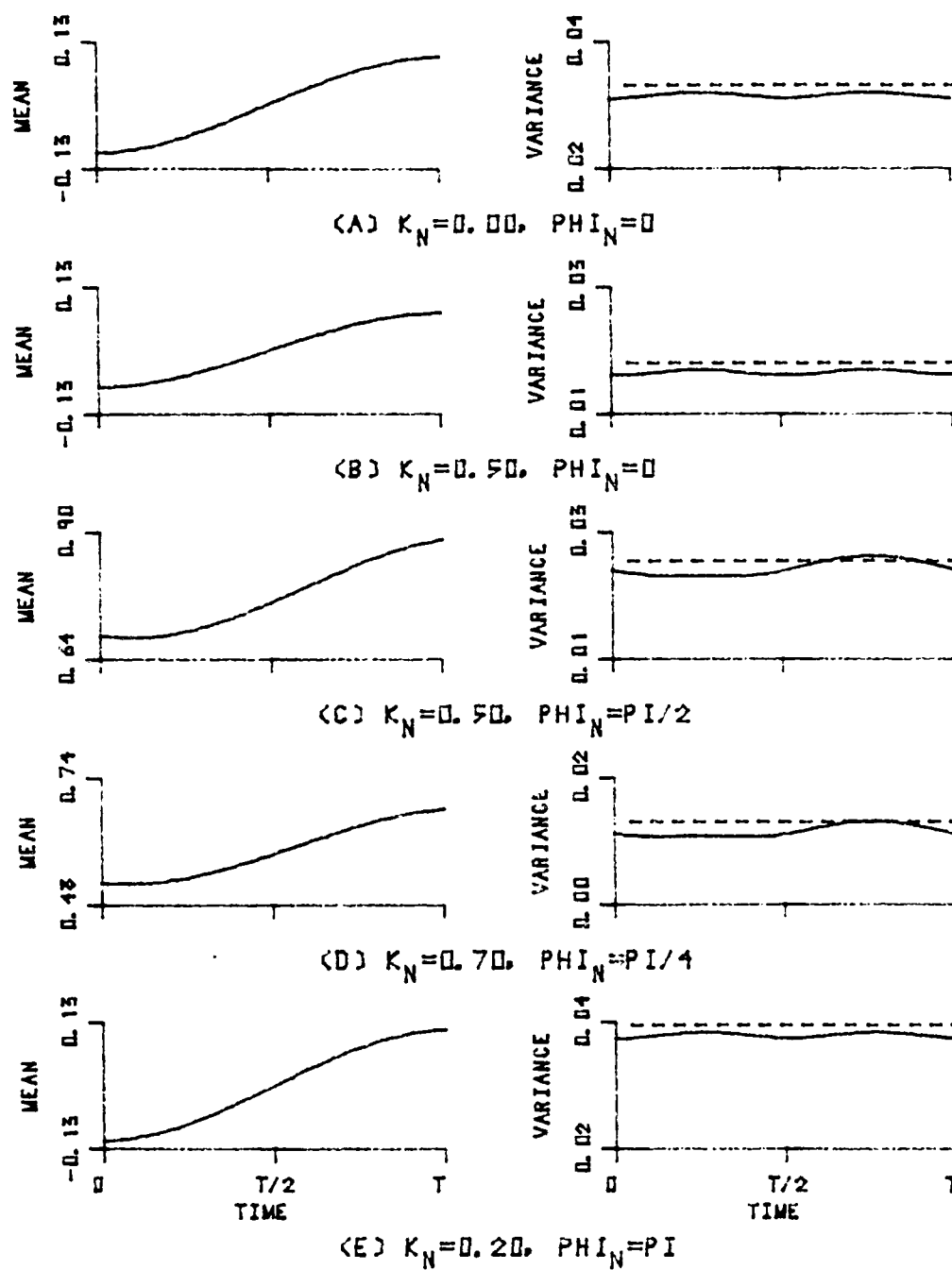


FIGURE 4-3. Mean and Variance of Angle Average Phase Estimate for Linear Delay and SNR = -12 dB.

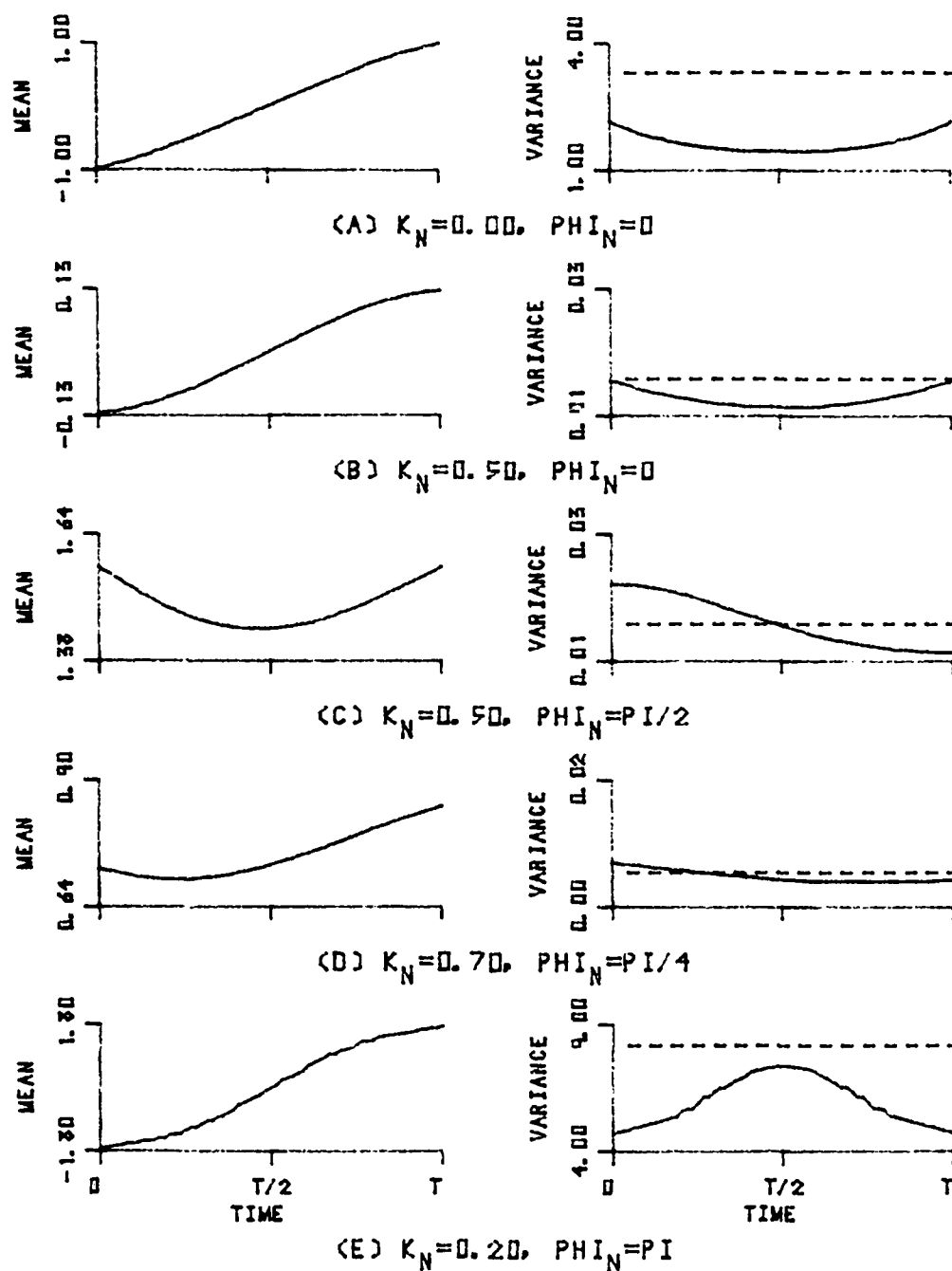


FIGURE 4-4. Mean and Variance of Vector Average Phase Estimate for Linear Delay and SNR = -12 dB.

$$\overline{\lambda}_T = \frac{1}{64} [-b_m(1) - \frac{1}{2} b_m(2) - \frac{1}{3} b_m(3)] \quad (4-4)$$

and the variance can be calculated assuming the average phase estimate is stationary with a variance equal to the average of the variance of the individual estimates over a processing interval.

$$\sigma_{\lambda}^2 \approx \frac{1}{2(64)^2} \frac{49}{36} c_v(0) \quad (4-5)$$

Equation (4-5) was used in calculating the ROC curves. In Figures 4-5 and 4-6, the ROC curves for a probability of false alarm of 10^{-3} and all noise correlation conditions are combined for angle average and vector average phase estimates, respectively. A comparison of the receiver performance as a function of noise correlation can be made. The variation in signal-to-noise ratio for a given p_D is less than 1.2 dB for the angle average case. The vector average method results in receiver performance which is more sensitive to noise correlation.

The ROC curves for the angle average phase estimate case can be further understood with the aid of Figure 4-3. The waveform shape of the mean of the average phase estimate remains highly linear over all the noise correlation conditions. The variance varies over a 3:1 range as the noise correlation changes but, in general, the peak-to-peak value of the mean increases as the variance increases. Thus, the detection performance when using angle average phase estimate is relatively insensitive to the noise correlation.

The detection performance when using the vector average phase estimate can be explained with the help of Figure 4-4. Consider first,

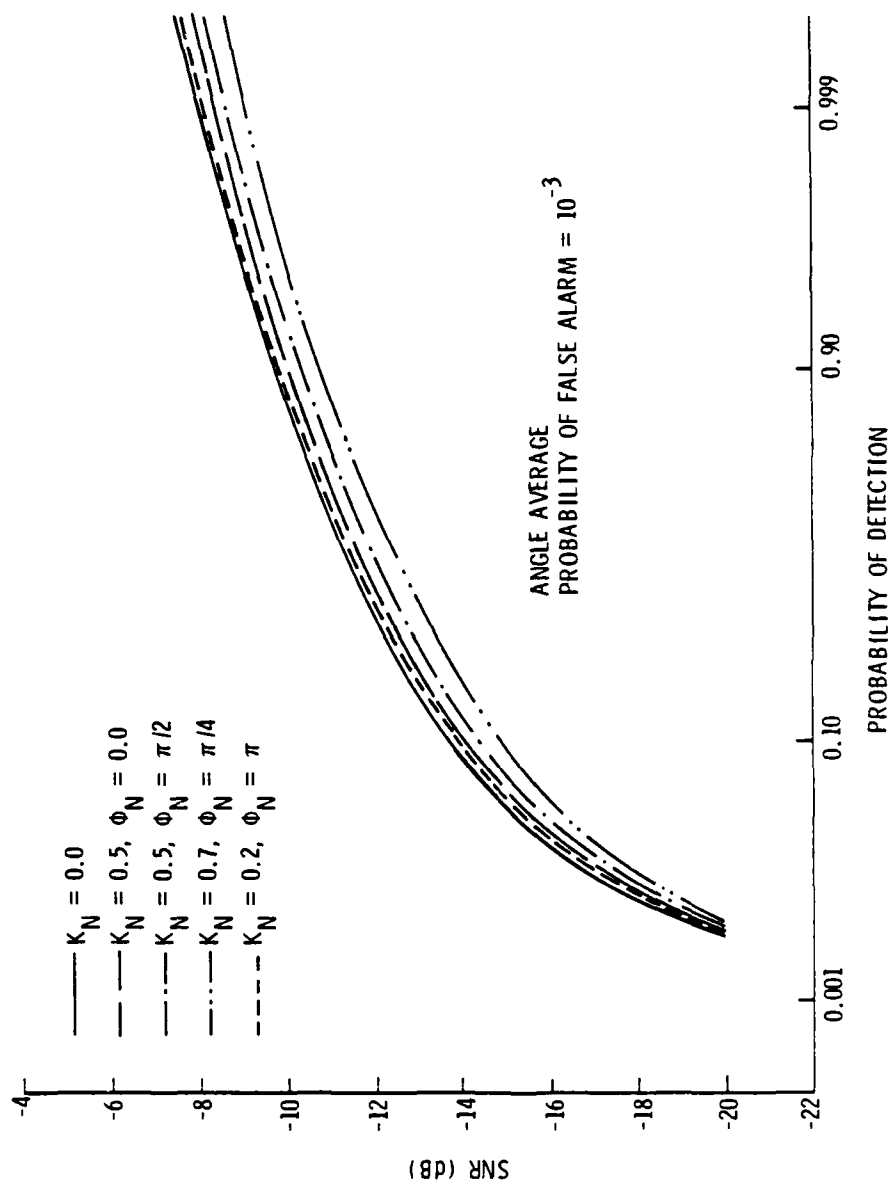


FIGURE 4-5. Detection Performance for Linear Delay and Angle Average Phase Estimate, Noise Correlation Known a Priori.

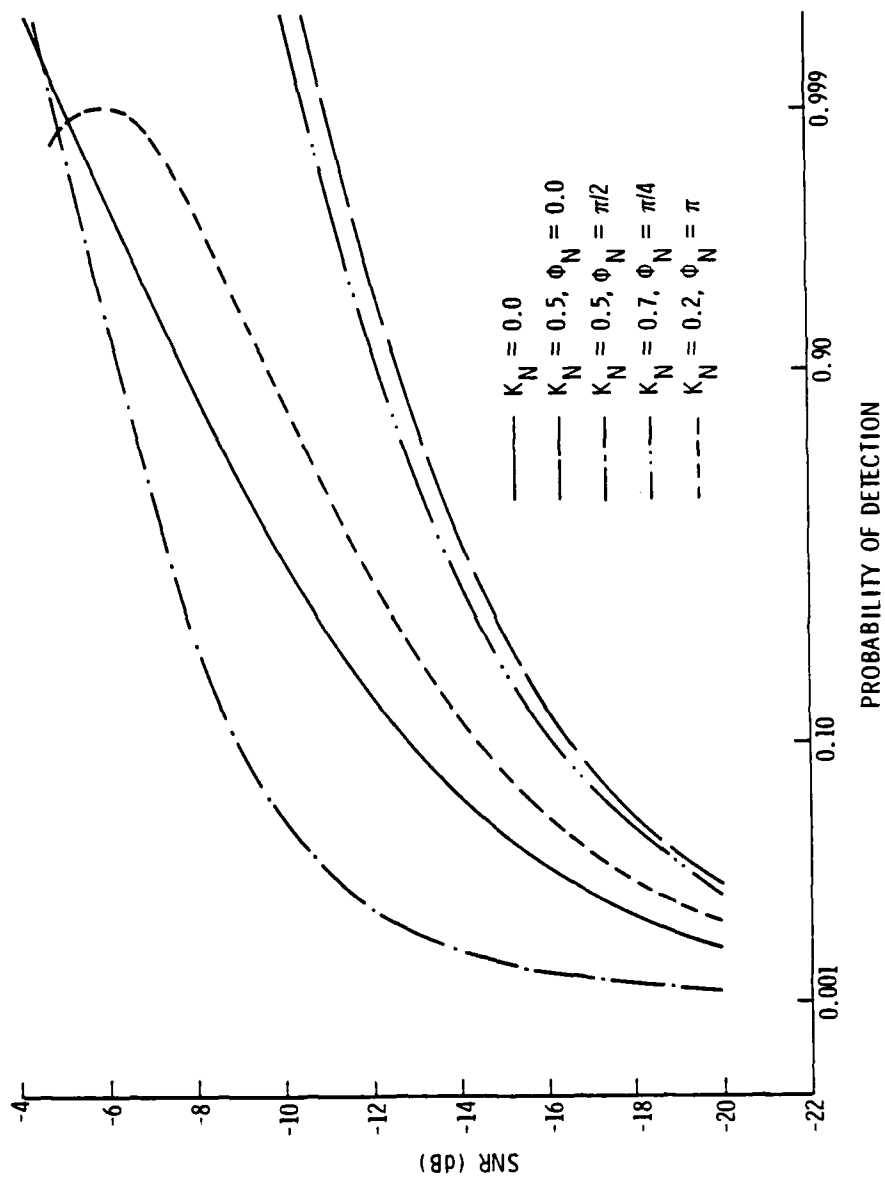


FIGURE 4-6. Detection Performance for Linear Delay and Vector Correlation Known a Priori.

the case of correlated noise, $K_N = 0.2$, $\phi_N = \pi$. The variance of the phase estimate is 2.86 when no signal is present. The standard deviation of the test statistic under the H_0 hypothesis is 0.295. At the high signal-to-noise ratio, the maximum peak value of the mean phase estimate is $\pi/2$. Thus, the maximum mean value of the test statistic is 0.458. In order to obtain a probability of false alarm of 10^{-3} , the threshold must be set 3.09 times the standard deviation or greater than maximum mean value of the test statistic. As the signal-to-noise ratio increases the variance and mean decreases and the probability of the test statistic exceeding the threshold decreases at signal-to-noise ratios greater than -6 dB. For probability of false alarm greater than 6×10^{-2} , the maximum mean value of the test statistic will exceed the threshold. This behavior could be avoided by increasing the number of points in the matched filter DFT.

Examination of mean phase estimate in Figure 4-4 shows the waveform is badly distorted for noise correlation of $K_N = 0.5$, $\phi_N = \pi/2$. With noise correlation phase of $\pi/2$ and signal-to-noise ratio less than the noise correlation magnitude, the mean vector average phase estimate waveform is no longer matched to the filter in the detector. As the signal-to-noise increases the mean vector average phase estimate waveform again becomes approximately linear. This noise ratio decreases in Figure 4-6 when the noise correlation phase is $\pi/2$.

4.2 Unknown Noise Correlation, Fixed Threshold Detector

Previously, it was assumed that the magnitude and phase of the noise correlation coefficient were known and the detector threshold could be set for a given probability of false alarm. It is also of interest to examine the case of a fixed threshold when the noise correlation is unknown.

Figures 4-7 and 4-8 are the receiver operating characteristics when the angle average method is used to estimate the average phase. The threshold was set to give a probability of false alarm of 10^{-3} ; in Figure 4-7 the threshold was set based on uncorrelated noise and in Figure 4-8 a noise correlation coefficient of $K_N = 0.5$, $\phi_N = 0$ was assumed. These curves can be compared directly with Figure 4-5 where the noise correlation was assumed known.

For the values of actual noise correlation considered in Figure 4-7, the worse case probability of false alarm would increase to 2.4×10^{-3} at a noise correlation of $K_N = 0.2$, $\phi_N = \pi$. For an actual noise correlation of $K_N = 0.5$, $\phi_N = 0$ or $K_N = 0.7$, $\phi_N = \pi/4$ the receiver sensitivity suffers a 1.1 dB loss. In Figure 4-8, the receiver sensitivity suffers no loss, but the probability of false alarm increases to 1.9×10^{-2} if the actual noise correlation were $K_N = 0.2$, $\phi_N = \pi$, the probability of false alarm would not exceed 10^{-3} for any of the actual cases considered and the loss of receiver sensitivity would be 1.8 dB. Thus, the performance of the receiver is relatively insensitive to noise correlation coefficient when using an angle average phase estimate and for the values of correlation considered.

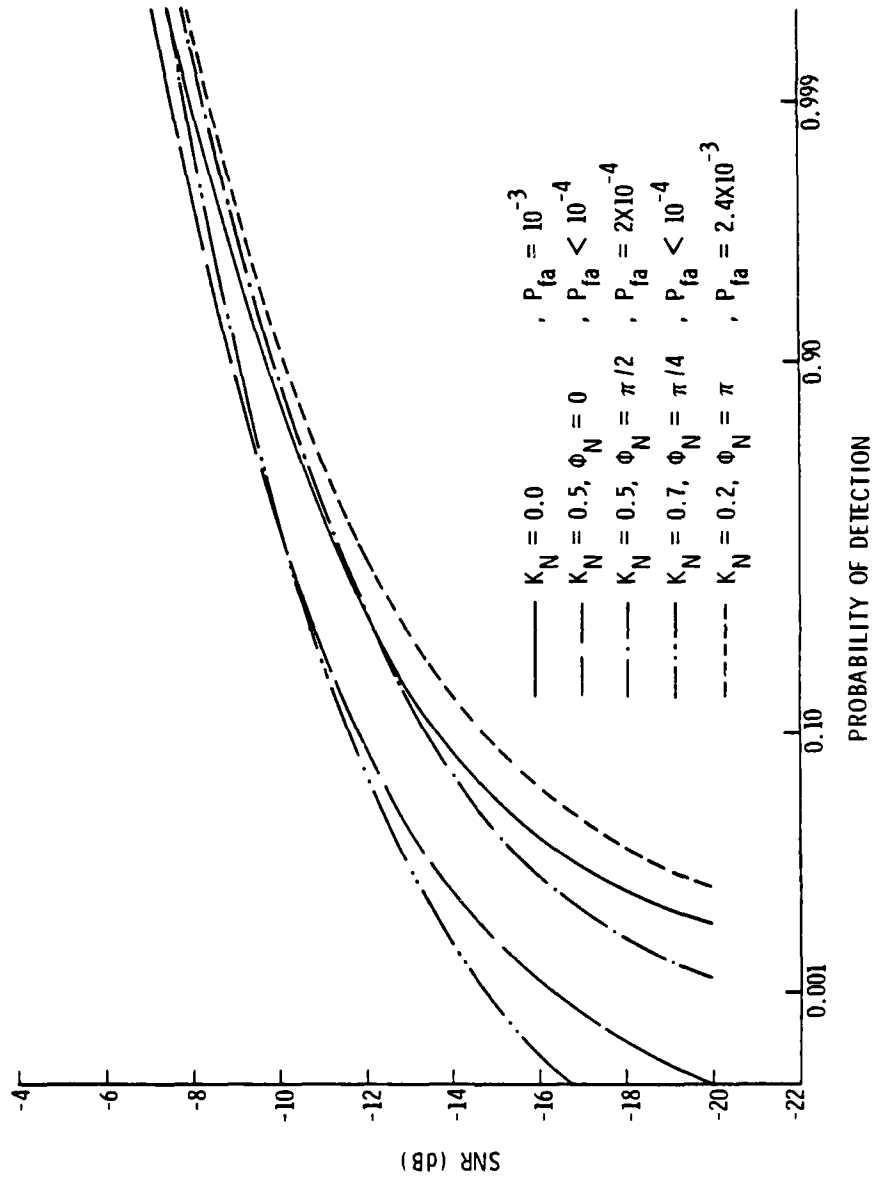


FIGURE 4-7. Detection Performance for Linear Delay, Angle Average Phase Estimate, Unknown Noise Correlation, and Threshold Set Assuming $K_N = 0.0$.

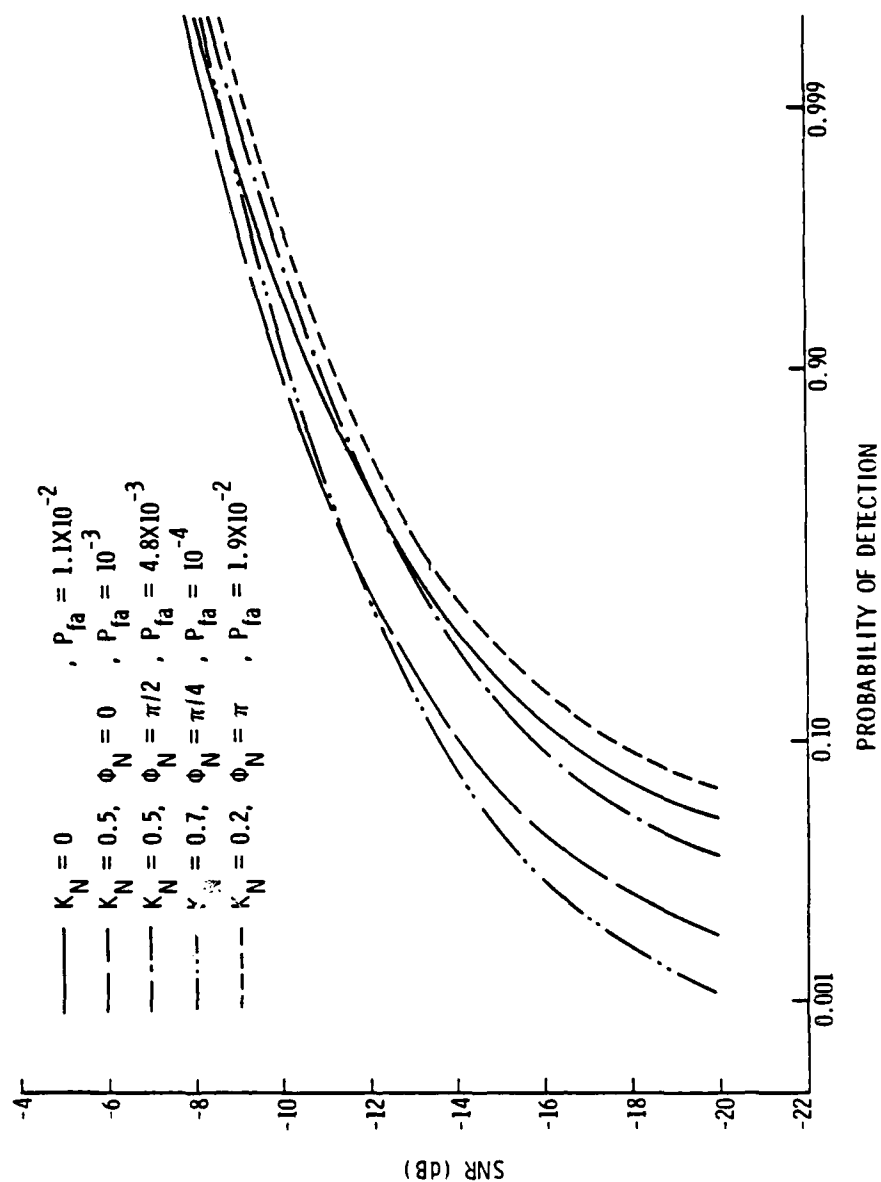


FIGURE 4-8. Detection Performance for Linear Delay, Angle Average Phase Estimate, Unknown Noise Correlation, and Threshold Set Assuming $K_N = 0.5$, $\phi_N = 0$.

The receiver operating characteristics when the vector average phase estimate is used are shown in Figures 4-9 and 4-10 for the same cases as considered previously. In Figures 4-9 and 4-10 the threshold was set assuming noise correlation of $K_N = 0.0$ and $K_N = 0.5$, $\phi_N = 0$, respectively. These receiver operating characteristics are sensitive to actual noise correlation coefficient. In Figure 4-9, the probability of false alarm increases to 2.5×10^{-3} for an actual noise correlation of $K_N = 0.2$, $\phi_N = \pi$. For other noise correlation conditions, the receiver sensitivity decreases such that for a signal-to-noise ratio of -4 dB the probability of detection is less than 10^{-4} . The curves in Figure 4-10 show a worse case decrease in expected receiver sensitivity of 6.8 dB while the probability of false alarm increases to 0.45 when the noise correlation is $K_N = 0.2$, $\phi_N = \pi$. It would be undesirable to use the vector average phase estimate if the noise correlation coefficient were not exactly known.

4.3 Comparison with Cross Correlation Detector

The cross correlation receiver is commonly used to detect Gaussian signals in Gaussian noise. To detect a dual channel, differential phase modulated signal in correlated noise, the cross correlator receiver includes a noise decorrelator or spatial pre-whitener and phase compensation. The detection performance of this cross correlation receiver is compared with the phase matched filter receiver for detection sensitivity and the sensitivity of the receivers to the noise correlation coefficient.

The cross correlation detector with spatial prewhitening and signal phase compensation is described in Appendix B. The necessary equations

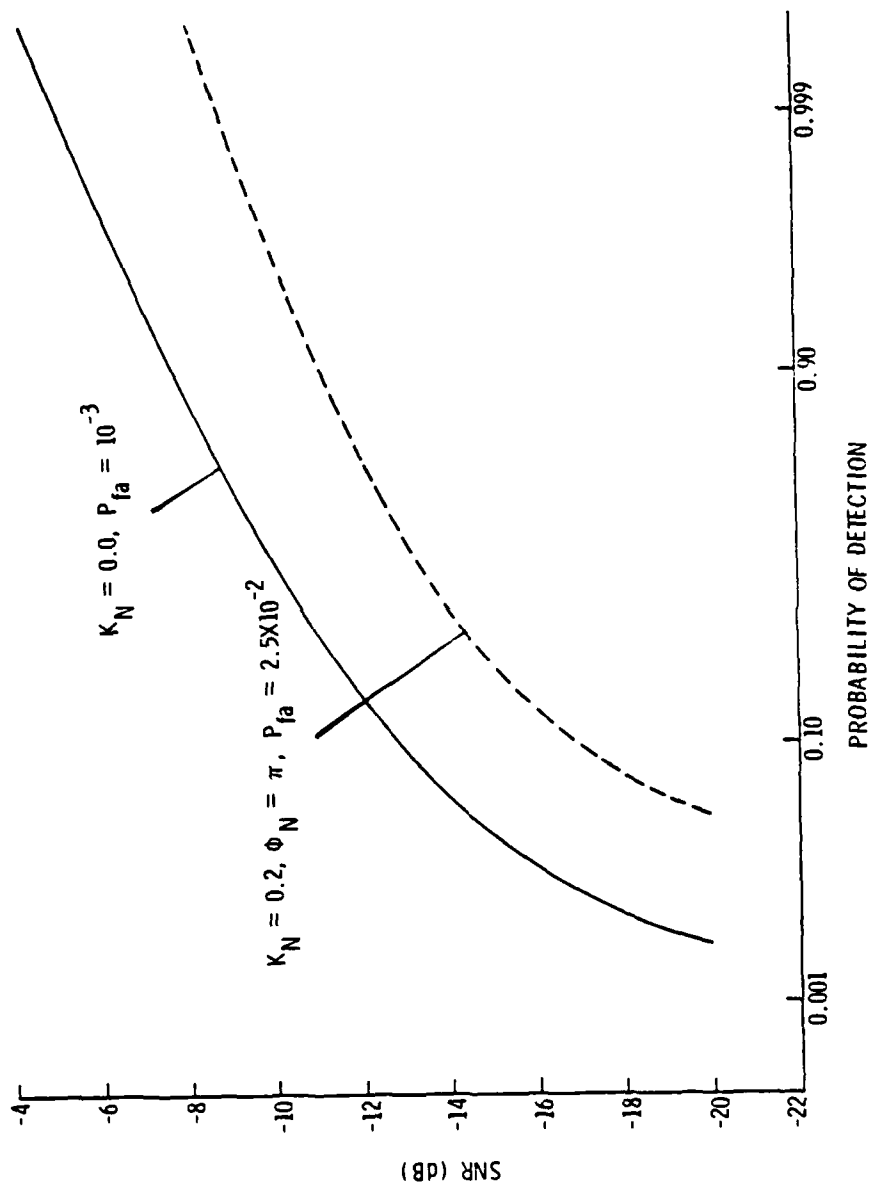


FIGURE 4-9. Detection Performance for Linear Delay, Vector Average Phase Estimate, Unknown Noise Correlation, and Threshold Set Assuming $K_N = 0$.

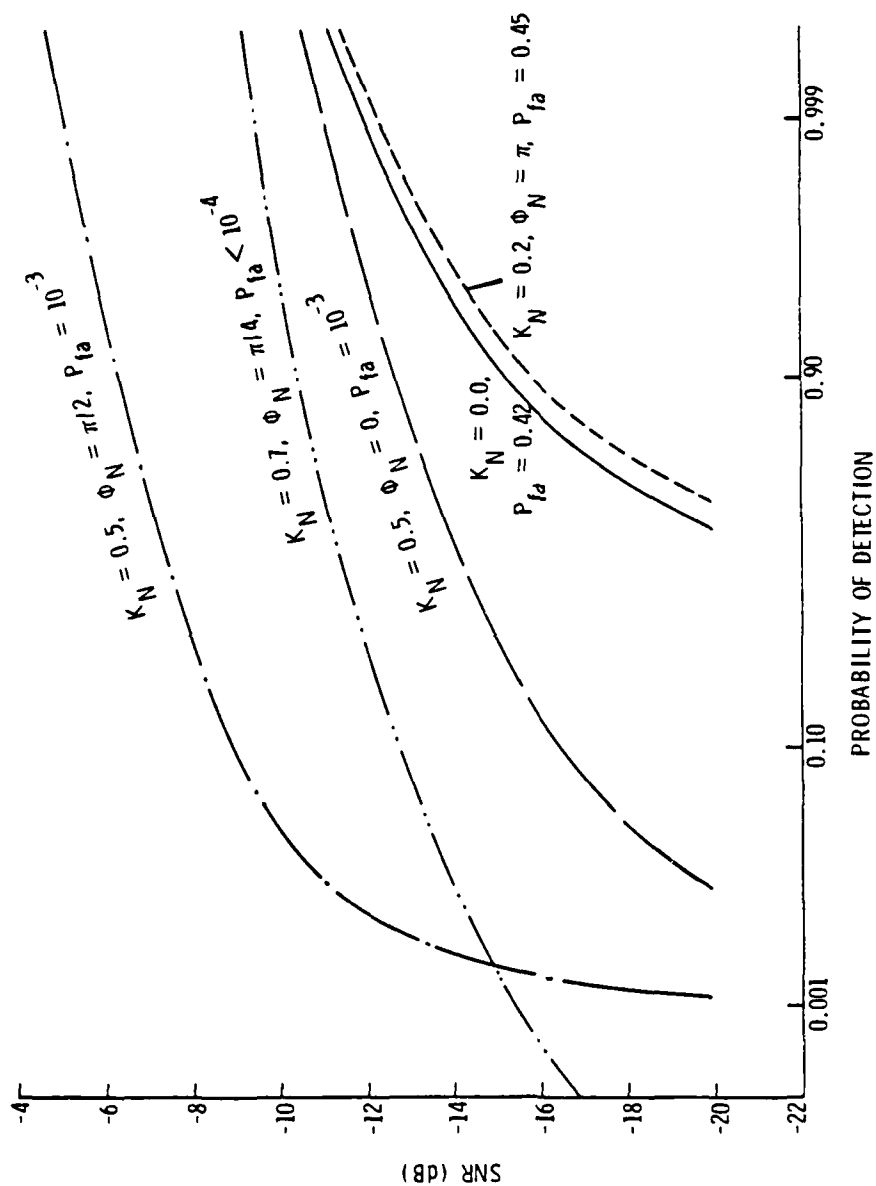


FIGURE 4-10. Detection Performance for Linear Delay, Vector Average Phase Estimate, Unknown Noise Correlation, and Threshold Set Assuming $K_N = 0.5, \phi_N = 0.0$

to calculate the receiver operating characteristic curves are also contained in Appendix B. The ROC curves for the linear time delay and a probability of false alarm of 10^{-3} were generated for two cases:

1) the noise correlation known, and 2) noise correlation unknown but threshold, prewhitening and phase compensation set assuming a noise correlation value. These ROC curves are compared with corresponding curves for the signal phase matched filter detector using either angle average or vector average phase estimation.

4.3.1 Known Noise Correlation

The ROC curves for a cross correlation detector using spatial prewhitening and signal phase compensation are shown in Figure 4-11. These curves represent the case when the threshold was set to give a probability of false alarm of 10^{-3} and thus correspond to the ROC curves in Figures 4-5 and 4-6 for the receiver using a signal phase matched filter. For the values of noise correlation considered, the cross correlation receiver using spatial prewhitening is 3.3 to 4.7 dB more sensitive than a receiver using angle average phase estimate and a phase matched filter detector. The cross correlation receiver is 0.7 to 8.8 dB more sensitive than a receiver using vector average phase estimate and a phase matched filter detector.

4.3.2 Unknown Noise Correlation

Two cases were examined for the cross correlation receiver with the spatial prewhitening, signal phase compensation and threshold set assuming a given noise correlation and the actual noise correlation

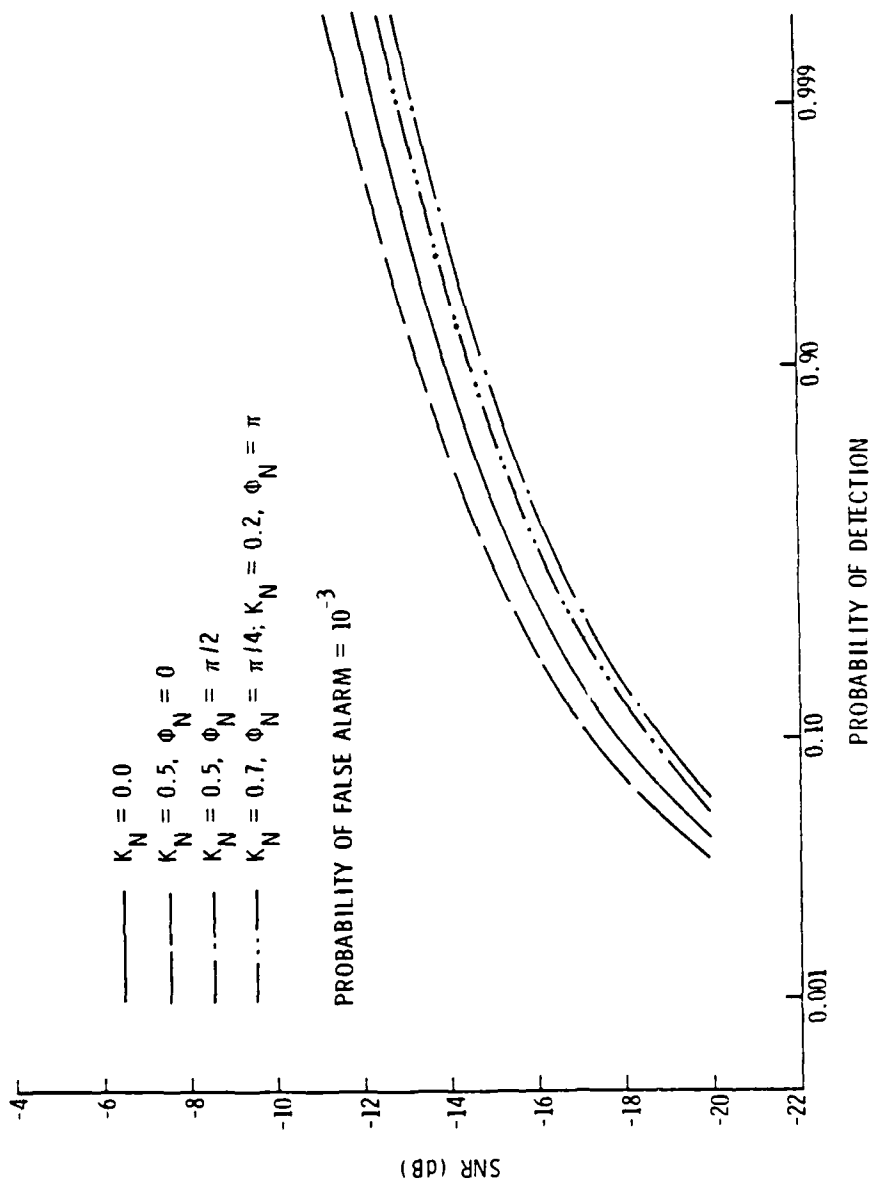


FIGURE 4-11. Detection Performance, Cross Correlation Receiver, Known Noise Correlation.

AD-A119 236

PENNSYLVANIA STATE UNIV UNIVERSITY PARK APPLIED RESE--ETC F/0 17/2
DETECTION OF A DUAL CHANNEL DIFFERENTIAL PHASE MODULATED SIGNAL--ETC(U)
JUN 82 C C MERCHANT
N00024-79-C-6043
ARL/PSU/TM-82-136

UNCLASSIFIED

NL

2 of 2

AD A
119236

END
DATE
FILMED

10-82
DTIC

being a different value. The ROC curves in Figures 4-12 and 4-13 are for assumed noise correlation of $K_N = 0.0$ and $K_N = 0.5$, $\phi_N = 0$, respectively. If the assumed noise is uncorrelated and the actual noise correlation is $K_N = 0.5$, $\phi_N = 0$; $K_N = 0.5$, $\phi_N = \pi/2$ or $K_N = 0.7$, $\phi_N = \pi/4$, the probability of detection will be greater than 0.9999. However, the probability of false alarm will also be greater than 0.9999. The same applies if the assumed noise correlation is $K_N = 0.5$, $\phi_N = 0$ and the actual noise correlation is $K_N = 0.2$, $\phi_N = \pi$. To reduce the probability of false alarm, it would be necessary to increase threshold and suffer the corresponding loss in sensitivity.

The ROC curves in Figures 4-12 and 4-13 can be compared directly with Figures 4-7 through 4-10 for the receivers using signal phase matched filter detector. The receiver which is least sensitive to the actual noise correlation is the receiver using angle average phase estimation and a signal phase matched filter.

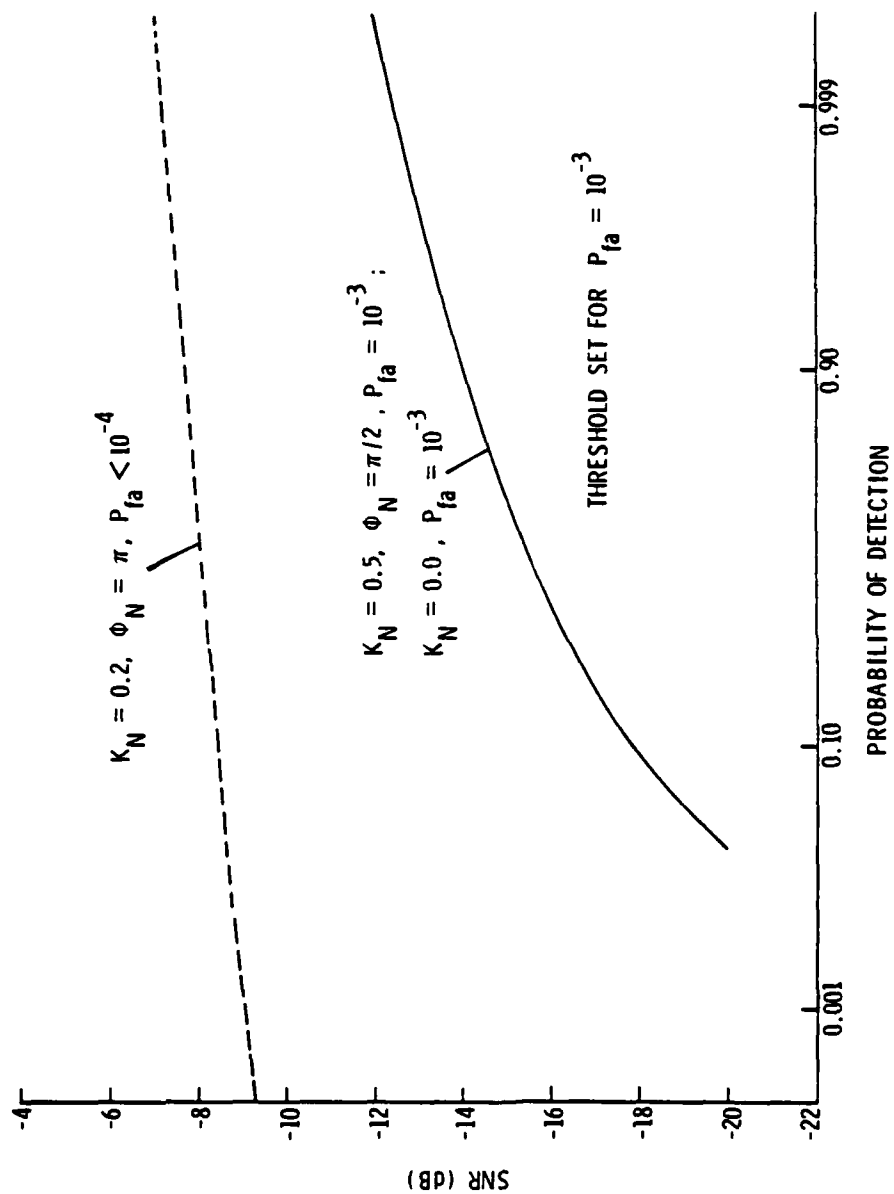


FIGURE 4-12. Detection Performance, Cross Correlation Receiver, Unknown Noise Correlation and Threshold Set Assuming $K_N = 0$.

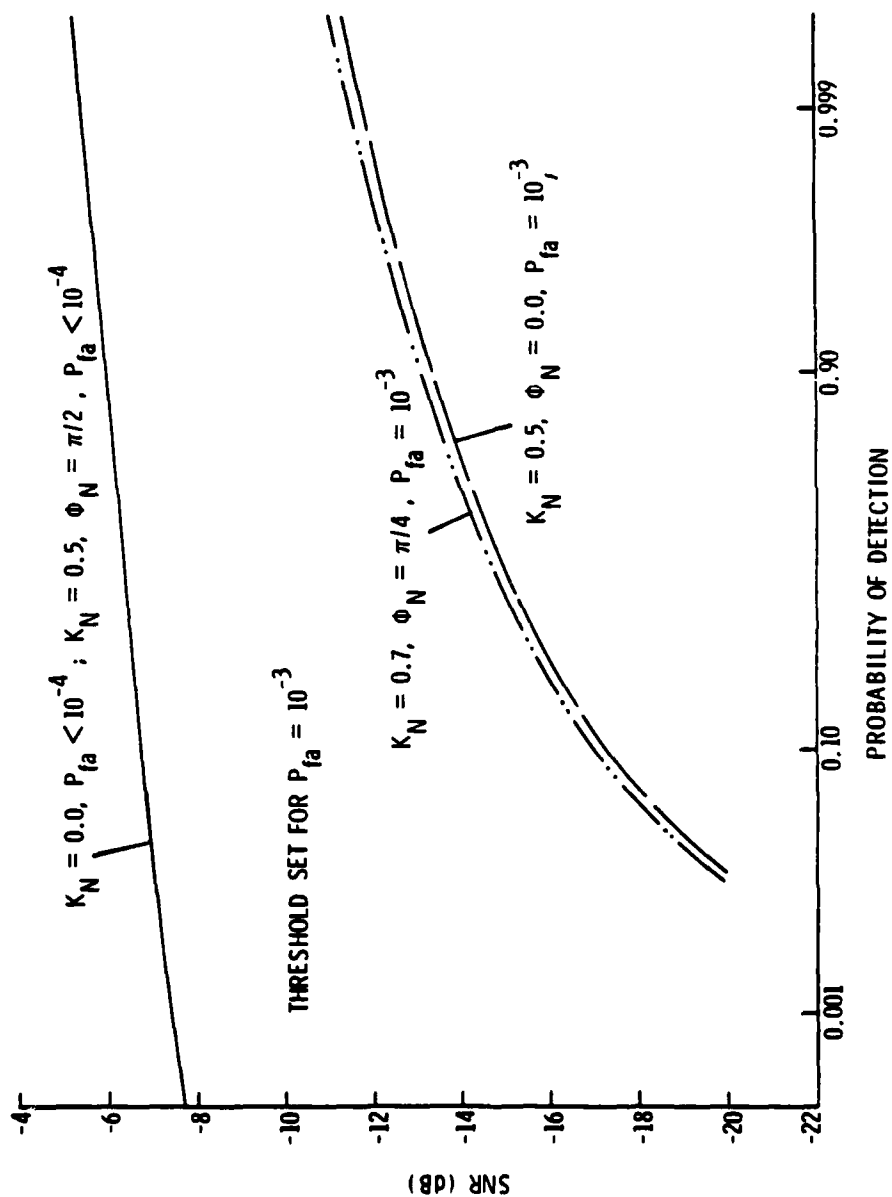


FIGURE 4-13. Detection Performance, Cross Correlation Receiver, Unknown Noise Correlation and Threshold Set Assuming $K_N = 0.5, \phi_N = 0$.

CHAPTER V

SUMMARY AND CONCLUSIONS

5.1 Summary

This research studied the signal detection characteristics of a receiver with two input channels. The signals received in both channels are random, narrowband processes which are identical except for a known, variable channel-to-channel time delay. The known time delay is represented by a carrier frequency phase shift when expressing the narrowband random signals. The noise is also a narrowband, random process. There can be correlation between the noise in each of the input channels.

Chapter II explained the generalized received signal and noise model and described the receiver being studied. The receiver estimates the average phase difference between the observable signals in each of the input channels. Methods of forming the average phase estimate considered are angle averaging and vector averaging. The average phase signal is passed through a filter whose transfer function is matched to the known time varying, signal phase. The filter is implemented using a discrete Fourier transform. The output of the filter is threshold detected to determine the presence of a signal with the known phase shift.

The theoretical statistics required to determine the detection performance of the receiver were developed in Chapter III. The statistics are functions of the input signal-to-noise ratio, the correlation of the noise in the two receiver input channels, the period of the phase averages and the number of points used in the discrete Fourier transform. The moments of the vector average phase estimate were derived. The variance of

the average phase signal varies with time; therefore, the moments of the Fourier coefficients were derived assuming a non-stationary periodic input. The receiver likelihood functions were determined so the probability of false alarm and probability of detection could be calculated.

In Chapter IV, the detection performance was determined for an example of possible signal phase shift function. The phase shift function considered was a linear phase shift. The receiver operating characteristic curves were generated for several noise correlation conditions assuming the noise correlation was known a priori. Finally, receiver operating characteristic curves were generated when the detection threshold was set for an assumed noise correlation but the actual noise correlation was not known a priori.

A performance comparison of the receiver using an average phase estimate and phase matched filter detector to a cross correlation detector was made. The cross correlation detector included a noise decorrelator and phase shift compensator. Comparisons were made assuming the noise correlation was known a priori and then assuming the threshold was set for a given noise correlation but the noise was not known a priori.

5.2 Conclusions

It was stated that the signal processing was intended to detect at low signal-to-noise ratios and over a variety of noise correlation values. The receiver proved to be robust under these conditions when the angle averaging method of estimating the average phase was used. For the noise correlation conditions investigated, the variation in signal-to-noise ratio for a given probability of detection was less 1.2 dB. The

performance when using the vector average phase estimate was more sensitive to the value of the noise correlation. When the noise correlation is known exactly a priori, the choice of phase averaging method depends on the exact value of the correlation and the desired probability of false alarm.

In the case of a fixed threshold based on an assumed value of noise correlation where the actual noise correlation is not known a priori, the performance using the vector average phase estimate is unsatisfactory. The variance of the test statistics and hence the threshold setting is sensitive to the actual value of the noise correlation. The angle average phase estimate is less sensitive to the actual value of the noise correlation. When the noise correlation is not known a priori and the angle average phase estimate is used, a threshold setting can be found which will give variation in signal-to-noise ratio of less than 6 dB for a given probability of detection and a probability of false alarm below a desired level. For the noise correlation values studied, the variation in signal-to-noise ratio for 50% probability of detection was 2 dB.

A comparison of a cross correlation receiver with noise decorrelator and phase compensator and a receiver using an average phase estimate and phase matched filter detector was made for the noise correlation known a priori and for a threshold based on an assumed noise correlation when the actual correlation was not known a priori. The cross correlation receiver is approximately 4 dB more sensitive than a receiver using an angle average phase estimator when the noise correlation is known a priori. The cross correlation receiver is 1 to 9 dB more sensitive than a receiver using an vector average phase estimator when the noise correlation is known a priori. If the noise correlation is not known a priori, the performance

of the cross correlation detector is unsatisfactory.

The major accomplishment of this research is the development of a receiver with fixed detection threshold and signal processing which will detect a differential phase modulated signal in correlated noise when the value of the noise correlation is unknown. The phase matched filter receiver with an angle average phase estimator can be used over a wide range of noise correlation values. Although it is not as sensitive as the cross correlation receiver under known noise conditions, its sensitivity does not degrade as much when the noise correlation is not known a priori.

5.3 Future Research

Several areas need further research to fully understand and optimize a receiver to detect a dual channel, differential phase shifted signal. Some of these topics are discussed briefly.

The detection of known signals was performed with a given phase averaging period and a given number of points in the discrete Fourier transform. No attempt was made to optimize these variables or the trade-off between them. A trade-off study should be performed to determine the total processing period and the division of the samples within the processing period between the phase averages and discrete Fourier transform.

The detection of known signals assumed a peak phase for the desired signal. In some systems, the magnitude of the peak phase may be a design parameter. The curves of the mean average phase have a peak at a value of signal phase that is a function of the signal-to-noise ratio and noise correlation coefficient. The presence of this peak implies that there may be a value peak signal phase that is optimum.

REFERENCES

¹D. Middleton, Introduction to Statistical Communications, McGraw-Hill, New York, 1961.

²P. M. Schultheiss and F. B. Tuteur, "Optimum and Suboptimum Detection of Directional Gaussian Signals in an Isotropic Gaussian Noise Field," IEEE Transactions on Military Electronics, Vol. MIL-9, pp. 197-208, July/October 1965.

³R. N. McDonough, "A Canonical Form of the Likelihood Detector for Gaussian Random Vectors," Journal of the Acoustical Society of America, Vol. 49, pp. 402-406, 1971.

⁴A. D. Whalen, Detection of Signals in Noise, Academic Press, New York, 1971, pp. 392-396.

⁵W. M. Siebert, "Some Applications of Detection Theory to Radar," 1958 National Convention Record, Pt. 4, pp. 5-14.

⁶F. B. Tuteur, "Detectability of Directional Amplitude-Modulated Noise Signals in an Isotropic Noise Background of Unknown Power Level," IEEE Transactions on Information Theory, Vol. IT-11, pp. 591-593, 1965.

⁷C. N. Knapp and G. Clifford Carter, "The Generalized Correlation Method for Estimation of Time Delay," IEEE Transactions on Acoustics, Speech and Signal Processing, Vol. ASSP-24, pp. 320-327, 1976.

⁸W. B. Adams, J. P. Kuhn, and W. P. Whyland, "Correlator Compensation Requirements for Passive Time-Delay Estimation with Moving Source or Receivers," IEEE Transactions on Acoustics, Speech and Signal Processing, Vol. ASSP-28, pp. 158-168, 1980.

⁹J. B. Thomas, An Introduction to Statistical Communication Theory, John Wiley and Son, New York, pp. 187-194.

¹⁰Whalen, pp. 132-135.

¹¹Whalen, pp. 52-82.

¹²Whalen, pp. 69-70.

¹³A. V. Oppenheim and R. W. Schaffer, Digital Signal Processing, Prentice-Hall, Inc., Englewood Cliffs, N.J., 1975, p. 365.

¹⁴Oppenheim and Schaffer, Chapter 3, pp. 87-121.

¹⁵A. J. Rainal, "Monopulse Radars Excited by Gaussian Signals," IEEE Transactions on Aerospace and Electronic Systems, AES-2, 1966, pp. 337-345.

¹⁶Personal communication with F. E. Fenlon, The Pennsylvania State University, Applied Research Laboratory, October 7, 1977.

¹⁷R. V. Hogg and A. T. Craig, Introduction to Mathematical Statistics, Macmillan Co., New York, 1965, p. 148.

APPENDIX A

SELECTED MIXED CENTRAL MOMENTS OF QUADRIVARIATE
GAUSSIAN DENSITY FUNCTION

The mean, variance, and covariance of the real and imaginary components of a product of two complex variables can be found from the appropriate mixed central moments of the joint density function of the components of the two complex variables. The product of a complex variable multiplied by the complex conjugate of the second complex variable is given by

$$\begin{aligned} uv^* &= (u_c + ju_s)(v_c - jv_s) \\ uv^* &= (u_c v_c + u_s v_s) + j(u_s v_c - u_c v_s). \end{aligned} \quad (A-1)$$

The real and imaginary components are:

$$x = \text{Re} [uv^*] = u_c v_c + u_s v_s \quad (A-2)$$

$$y = \text{Im} [uv^*] = u_s v_c - u_c v_s \quad (A-3)$$

The mean, variance, and covariance values can be obtained from the mixed central moments of the joint probability distribution of the variables u_c , u_s , v_c , and v_s .

The variables u_c , u_s , v_c , and v_s are zero mean Gaussian variables, described by covariance matrix:

$$R = [E \{ \underline{Z} \underline{Z}' \}] \quad (A-4)$$

where the vector \underline{Z} is related to the variables u_c , u_s , v_c , and v_s by

$$\underline{Z} = \begin{bmatrix} z_1 \\ z_2 \\ z_3 \\ z_4 \end{bmatrix} = \begin{bmatrix} u_c \\ u_s \\ v_c \\ v_x \end{bmatrix} \quad (\text{A-5})$$

The i th term of R is equal to the j th term so that the covariance matrix is symmetric. The quadrivariate Gaussian density function is given by

$$P(\underline{Z}) = \frac{1}{(2\pi)^2 |R|^{1/2}} \exp \left(-\frac{1}{2} \underline{Z}' R^{-1} \underline{Z} \right) \quad (\quad)$$

and the characteristic function is

$$C(j\underline{\omega}) = e^{-\frac{1}{2} \underline{\omega}' R \underline{\omega}} \quad (\text{A-7})$$

or

$$C(j\underline{\omega}) = \exp \left\{ -\frac{1}{2} \sum_{i=1}^4 \sum_{k=1}^4 \omega_k r_{ki} \omega_i \right\} \quad (\text{A-8})$$

where

$$r_{ij} = E \{ Z_i Z_j \}$$

$$\underline{\omega} = [\omega_1, \omega_2, \omega_3, \omega_4]'$$

The mixed moment $E\{x_1^{b_1} x_2^{b_2} x_3^{b_3} x_4^{b_4}\}$ where b_i are positive integers can be found from

$$E\{z_1^{b_1} z_2^{b_2} z_3^{b_3} z_4^{b_4}\} = \frac{1}{a^{B/2} (B/2)!} \frac{\partial^B}{\partial \omega_1^{b_1} \partial \omega_2^{b_2} \partial \omega_3^{b_3} \partial \omega_4^{b_4}} \\ \times \left[\sum_{i=1}^4 \sum_{k=1}^4 \omega_k r_{ki} \omega_i \right]^{B/2} \bigg|_{\substack{\omega_i=0 \\ \omega_k=0}} \quad (A-9)$$

where

$$B = b_1 + b_2 + b_3 + b_4$$

Of interest in finding the mean, variance, and covariance are terms of the form $E\{z_i z_j\}$, $E\{z_i^2 z_j^2\}$, $E\{z_1 z_2 z_3 z_4\}$ and $E\{z_i^2 z_j z_k\}$. The first term is:

$$E\{z_i z_j\} = r_{ij} \quad (A-10)$$

$E\{z_i^2 z_j^2\}$ is given by

$$E\{z_i^2 z_j^2\} = \frac{1}{8} \frac{\partial^4}{\partial \omega_i^2 \partial \omega_j^2} \left[\sum_{i=1}^4 \sum_{j=1}^4 \omega_i r_{ij} \omega_j \right]^2 \bigg|_{\omega_i=0}$$

The only terms which will not be zero are those terms of the form

$\omega_i^2 \omega_j^2$. . ., therefore,

$$E\{z_i^2 z_j^2\} = r_{ii} r_{jj} + 2 r_{ij}^2 \quad (A-11)$$

Similarly for $E\{z_i^2 z_j z_k\}$, the only non-zero term are of the form $\omega_i^2 \omega_j \omega_k \dots$ therefore,

$$E\{w_i^2 w_j w_k\} = r_{ii} r_{jk} + 2 r_{ij} r_{ik} \quad (\text{A-12})$$

and

$$E\{z_1 z_2 z_3 z_4\} = r_{12} r_{34} + r_{13} r_{24} + r_{14} r_{23} \quad (\text{A-13})$$

The terms of interest are:

$$\left. \begin{aligned} E\{u_c v_c\} &= r_{13} \\ E\{u_c v_s\} &= r_{14} \\ E\{u_s v_c\} &= r_{23} \\ E\{u_s v_s\} &= r_{24} \\ E\{u_c^2 v_c^2\} &= r_{11} r_{33} + 2 r_{13}^2 \\ E\{u_c^2 v_s^2\} &= r_{11} r_{44} + 2 r_{14}^2 \\ E\{u_s^2 v_c^2\} &= r_{22} r_{33} + 2 r_{23}^2 \\ E\{u_s^2 v_s^2\} &= r_{22} r_{44} + 2 r_{24}^2 \\ E\{u_c^2 v_c v_s\} &= r_{11} r_{34} + 2 r_{13} r_{14} \\ E\{u_s^2 v_c v_s\} &= r_{22} r_{34} + 2 r_{23} r_{24} \\ E\{u_c u_s v_c^2\} &= r_{33} r_{12} + 2 r_{13} r_{23} \\ E\{u_c u_s v_s^2\} &= r_{44} r_{12} + 2 r_{14} r_{24} \end{aligned} \right\} \quad (\text{A-14})$$

Using equations (A-13) and (A-14), the moments of the real and imaginary components are:

$$\bar{x} = r_{13} + r_{24} \quad (\text{A-15})$$

$$\bar{y} = r_{23} - r_{14} \quad (\text{A-16})$$

$$\sigma_x^2 = r_{11} r_{33} + r_{22} r_{44} + r_{13}^2 + r_{24}^2 + 2 r_{14} r_{23} + 2 r_{12} r_{34} \quad (\text{A-17})$$

$$\sigma_y^2 = r_{11} r_{44} + r_{22} r_{33} + r_{14}^2 - r_{23}^2 + 2 r_{13} r_{24} + 2 r_{12} r_{34} \quad (\text{A-18})$$

$$\mu_{xy} = (r_{13} + r_{24}) (r_{23} - r_{14}) + r_{12} (r_{33} - r_{44}) + r_{34} (r_{22} - r_{11}) \quad (\text{A-19})$$

APPENDIX B

NOISE DECORRELATOR, SIGNAL PHASE COMPENSATION,
CROSS CORRELATION RECEIVER

The cross correlation receiver is shown in Figure B-1. The observable signals are processed by a noise decorrelator and phase compensator. The signal processing is then split into two channels. The first channel estimates the covariance and the second channel estimates the power level. The weighted differences of the two processing channels is formed.

If the weighted difference is positive, the signal present hypothesis is selected.

Noise Decorrelator

The transfer function of the noise decorrelator is:

$$H_D = \begin{bmatrix} 1 & 0 \\ \frac{-\hat{K}_N e^{-j\hat{\phi}_N}}{\sqrt{1-\hat{K}_N^2}} & -\frac{1}{\sqrt{1-\hat{K}_N^2}} \end{bmatrix} \quad (B-1)$$

where \hat{K}_N and $\hat{\phi}_N$ are the estimated magnitude and phase of the noise correlator and coefficient. The covariance matrix of the input signals is:

$$R_r = \sigma_o^2 \begin{bmatrix} 1 & K_o e^{j\phi_o} \\ K_o e^{-j\phi_o} & 1 \end{bmatrix} \quad (B-2)$$

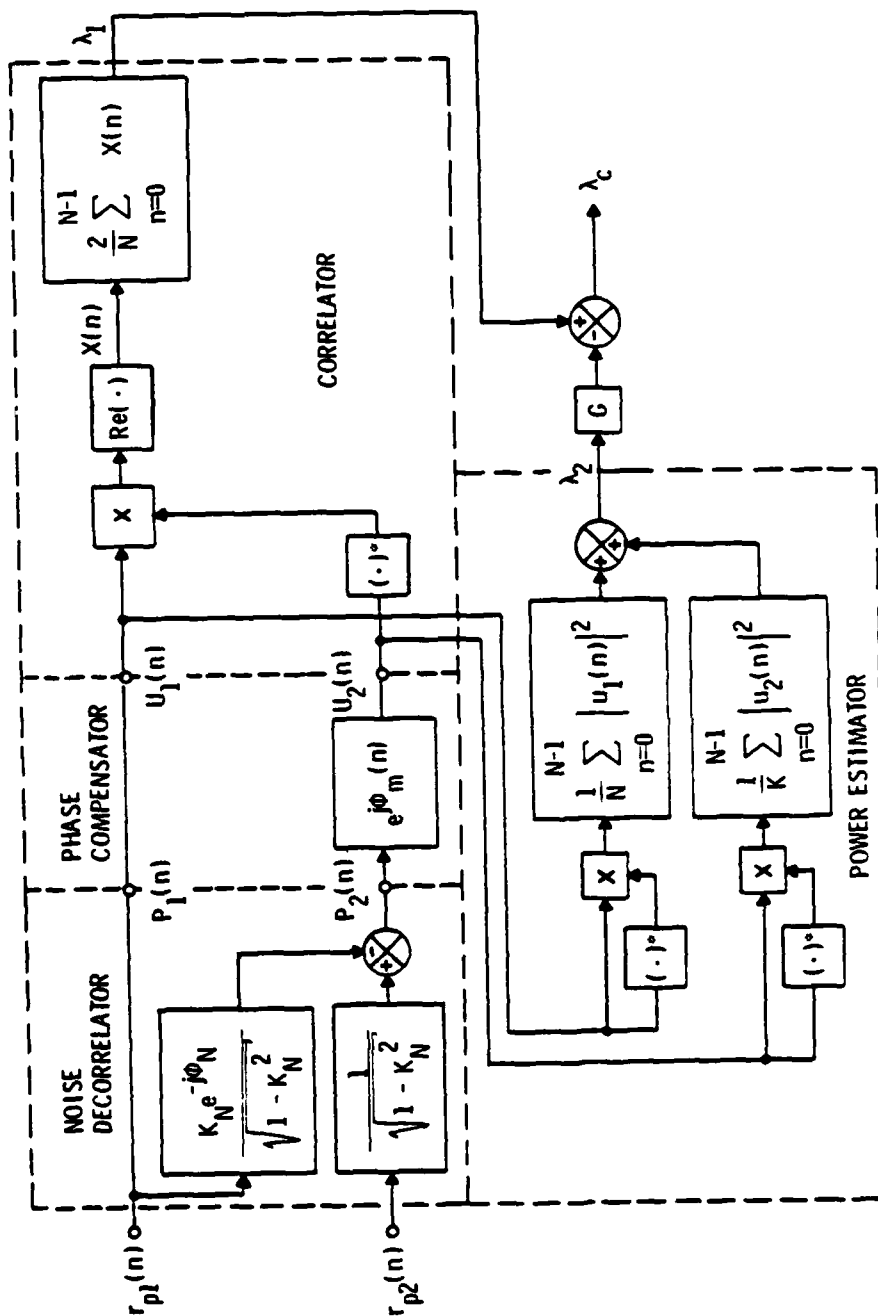


FIGURE B-1. Cross Correlation Receiver.

The covariance matrix at the output of the decorrelator is:

$$R_p = H_D R_r H_D^+ \quad (B-3)$$

$$R_p = \sigma_o^2 \begin{bmatrix} 1 & \frac{K_o e^{j\phi_o} - \hat{K}_N e^{j\phi_N}}{\sqrt{1 - \hat{K}_N^2}} \\ \frac{K_o e^{-j\phi_o} - \hat{K}_N e^{-j\phi_N}}{\sqrt{1 - \hat{K}_N^2}} & \frac{1 + \hat{K}_N^2 - 2K_o \hat{K}_N \cos(\phi_o - \phi_N)}{1 - \hat{K}_N^2} \end{bmatrix}$$

For signal-plus-noise with the decorrelator and noise matched, the covariance matrix at the output of the decorrelator is:

$$R_p|_{s+n} = \sigma_N^2 \begin{bmatrix} 1 + h & \frac{h K_m e^{j\phi_m}}{\sqrt{1 - K_N^2}} \\ \frac{h K_m e^{-j\phi_m}}{\sqrt{1 - K_N^2}} & 1 + \frac{h K_m^2}{1 - K_N^2} \end{bmatrix} \quad (B-4)$$

where

$$K_m = \left[(\cos \phi_s - \hat{K}_N \cos \hat{\phi}_N)^2 + (\sin \phi_s - \hat{K}_N \sin \hat{\phi}_N)^2 \right]^{1/2} \\ = \left[1 + \hat{K}_N^2 - 2 \hat{K}_N \cos (\phi_s - \hat{\phi}_N) \right]^{1/2} \quad (B-5)$$

$$\phi_m = \tan^{-1} \left(\frac{\sin \phi_s - \hat{K}_N \sin \hat{\phi}_N}{\cos \phi_s - \hat{K}_N \cos \hat{\phi}_N} \right) \quad (B-6)$$

Phase Compensation

The phase compensation operates on the observable signal to cause the covariance terms to be real. This is accomplished with the transfer function:

$$H_m = \begin{bmatrix} 1 & 0 \\ 0 & e^{j\phi_m} \end{bmatrix} \quad (B-7)$$

The general covariance matrix at the output of the phase compensator is:

$$R_u = H_m R_p H_m^+ \quad (B-8)$$

$$R_u = \sigma_o^2 \begin{bmatrix} 1 & \frac{(K_o e^{j\phi_o} - \hat{K}_N e^{j\hat{\phi}_N}) e^{-j\phi_m}}{\sqrt{1 - \hat{K}_N^2}} \\ \frac{(K_o e^{-j\phi_o} - \hat{K}_N e^{-j\hat{\phi}_N}) e^{j\phi_m}}{\sqrt{1 - \hat{K}_N^2}} & \frac{1 + \hat{K}_N^2 - 2K_o \hat{K}_N \cos(\phi_o - \hat{\phi}_N)}{1 - \hat{K}_N^2} \end{bmatrix}$$

For the signal-plus-noise case, R_u becomes:

$$R_u|_{s+n} = \sigma_N^2 \begin{bmatrix} 1 + h & \frac{h K_m}{\sqrt{1 - \hat{K}_N^2}} \\ \frac{h K_m}{\sqrt{1 - \hat{K}_N^2}} & 1 + \frac{h K_m^2}{1 - \hat{K}_N^2} \end{bmatrix} \quad (B-9)$$

The signal phase is a time varying function. The time delay compensation then must also be a function of time. If R_u is put in terms of the real and imaginary components of u the isomorphic counterpart for the general covariance matrix becomes:

$$R_u = \sigma_o^2 \begin{bmatrix} 1 & 0 & \rho_u & -\lambda_u \\ 0 & 1 & \lambda_u & \rho_u \\ \rho_u & \lambda_u & \alpha_u^2 & 0 \\ -\lambda_u & \rho_u & 0 & \alpha_u^2 \end{bmatrix} \quad (B-10)$$

where

$$\alpha_u^2 = \frac{1 + \hat{K}_N^2 - 2 K_o \hat{K}_N \cos(\phi_o - \hat{\phi}_N)}{1 - \hat{K}_N^2} \quad (B-11)$$

$$\rho_u = \text{Re} \left[\frac{(K_o e^{j\phi_o} - \hat{K}_N e^{j\hat{\phi}_N}) e^{-j\phi_m}}{\sqrt{1 - \hat{K}_N^2}} \right] \quad (B-12)$$

$$\lambda_u = \text{Im} \left[\frac{(K_o e^{j\phi_o} - \hat{K}_N e^{j\hat{\phi}_N}) e^{-j\phi_m}}{\sqrt{1 - \hat{K}_N^2}} \right] \quad (B-13)$$

Covariance Estimator

The covariance estimator performs the operation:

$$\lambda_1 = \frac{2}{N} \sum_{n=0}^{N-1} x(n) \quad (B-14)$$

where

$$x(n) = \text{Re} \{u_1(n) u_2^*(n)\} \quad (\text{B-15})$$

The mean and variance of x can be found from the expression developed in Appendix A.

$$\bar{x} = 2 \sigma_o^2 \rho_u \quad (\text{B-16})$$

$$\sigma_x^2 = 2 \sigma_o^4 (\alpha_u^2 + \rho_u^2 - \lambda_u^2) \quad (\text{B-17})$$

The x variable is averaged to form an estimate of the covariance.

The covariance estimate λ_1 is Gaussian distributed with a mean and variance

$$\bar{\lambda}_1 = \frac{4\sigma_o^2}{N} \sum_{n=0}^{N-1} \rho_u(n) \quad (\text{B-18})$$

$$\sigma_1^2 = \frac{8\sigma_o^4}{N^2} \sum_{n=0}^{N-1} [\alpha_u^2(n) + \rho_u^2(n) - \lambda_u^2(n)] \quad (\text{B-19})$$

Power Estimator

The power level estimate is:

$$\lambda_2 = \frac{1}{N} \sum_{n=0}^{N-1} u_1(n) u_1^*(n) + \frac{1}{N} \sum_{n=0}^{N-1} u_2(n) u_2^*(n) \quad (\text{B-20})$$

The power level estimator is assumed to be Gaussian with mean and variance:

$$\bar{\lambda}_2 = 2 \sigma_o^2 \left(1 + \frac{1}{N} \sum_{n=0}^{N-1} \alpha_u^2(n) \right) \quad (\text{B-21})$$

$$\sigma_2^2 = \frac{4\sigma_o^4}{N} \left\{ 1 + \frac{1}{N} \sum_{n=0}^{N-1} \left[\alpha_u^4(n) + 2 \rho_u^2(n) + 2 \lambda_u^2(n) \right] \right\}. \quad (B-22)$$

The covariance between the power level estimate and the covariance estimate is:

$$\mu_\lambda = \frac{8\sigma_o^4}{N} \frac{1}{N} \sum_{n=0}^{N-1} \left[\rho_u(n) \left(1 + \alpha_u^2(n) \right) \right] \quad (B-23)$$

Test Statistic

The test statistic is the weighted difference of the covariance estimate and the power level estimate

$$\lambda_c = \lambda_1 - G\lambda_2. \quad (B-24)$$

The mean variance of the test statistic is:

$$\bar{\lambda}_c = 2\sigma_o^2 \left\{ \frac{2}{N} \sum_{n=0}^{N-1} \rho_u(n) - G \left[1 + \frac{1}{N} \sum_{n=0}^{N-1} \alpha_u^2(n) \right] \right\} \quad (B-25)$$

$$\begin{aligned} \sigma_c^2 = \frac{4\sigma_o^4}{N} \left\{ \frac{2}{N} \sum_{n=0}^{N-1} \left[\alpha_u^2(n) + \rho_u^2(n) - \lambda_u^2(n) \right] \right. \\ \left. + G^2 + \frac{G^2}{N} \sum_{n=1}^{N-1} \left[\alpha_u^2(n) + 2 \rho_u^2(n) + 2 \rho_u^2(n) \right] \right. \\ \left. - \frac{4G}{N} \sum_{n=0}^{N-1} \rho_u(n) \left[1 + \alpha_u^2(n) \right] \right\}. \quad (B-26) \end{aligned}$$

For the case of noise only and the noise and decorrelator are perfectly matched, the mean and variance is:

$$\bar{\lambda}_c \Big|_n = -4\sigma_N^2 G \quad (B-27)$$

$$\sigma_c^2 \Big|_n = \frac{8\sigma_N^4}{N} (1 + G^2) \quad (B-28)$$

The signal present hypothesis is selected if the test statistic is greater than zero. The probability of false alarm is given by

$$P_{fa} = \frac{1}{2} \left[1 - \operatorname{erf} \left(\frac{-\lambda_c \Big|_n}{\sqrt{2} \sigma_c \Big|_n} \right) \right]$$

$$P_{fa} = \frac{1}{2} \left[1 - \operatorname{erf} \left(\frac{\sqrt{2N} G}{\sqrt{2} \sqrt{1+G^2}} \right) \right] \quad (B-29)$$

The probability of detection is given by:

$$P_{fa} = \frac{1}{2} \left[1 - \operatorname{erf} \left(\frac{-\lambda_c \Big|_{s+n}}{\sqrt{2} \sigma_c \Big|_{s+n}} \right) \right] \quad (B-30)$$

DISTRIBUTION LIST FOR TM 82-136

Commander (NSEA 0342)
Naval Sea Systems Command
Department of the Navy
Washington, DC 20362

Copies 1 and 2

Commander (NSEA 9961)
Naval Sea Systems Command
Department of the Navy
Washington, DC 20362

Copies 3 and 4

Defense Technical Information Center
5010 Duke Street
Cameron Station
Alexandria, VA 22314

Copies 5 through 10